Printable Cement-Based Materials

Fresh Properties Measurements and Control

Wangler, Timothy; Flatt, Robert J.; Roussel, Nicolas; Perrot, Arnaud; Sonebi, Mohammed; Wolfs, Rob; Bos, Freek; Lowke, Dirk; Grünewald, Steffen; More Authors

DOI
10.1007/978-3-030-90535-4_4

Publication date
2022

Document Version
Final published version

Published in
Digital Fabrication with Cement-Based Materials: State-of-the-Art Report of the RILEM TC 276-DFC

Citation (APA)
Wangler, T., Flatt, R. J., Roussel, N., Perrot, A., Sonebi, M., Wolfs, R., Bos, F., Lowke, D., Grünewald, S., & More Authors (2022). Printable Cement-Based Materials: Fresh Properties Measurements and Control. In N. Roussel, & D. Lowke (Eds.), *Digital Fabrication with Cement-Based Materials: State-of-the-Art Report of the RILEM TC 276-DFC* (pp. 99-136). Springer. https://doi.org/10.1007/978-3-030-90535-4_4

Chapter 4
Printable Cement-Based Materials: Fresh Properties Measurements and Control

Timothy Wangler, Robert J. Flatt, Nicolas Roussel, Arnaud Perrot, Mohammed Sonebi, Rob Wolfs, Freek Bos, Dirk Lowke, Niklas Freund, Dietmar Stephan, Ursula Pott, Lex Reiter, Steffen Grünewald, Wilson Ricardo Leal da Silva, and Geert De Schutter

4.1 Introduction

Digital fabrication with cementitious materials is a fast-developing field, and advances have been particularly rapid within the past half decade. Cementitious materials are widely used in construction due to the wide availability of the raw materials, the relative ease of production, processing and handling, and especially the ability to transform from a fluid material that can fill a mould to a solid material that can bear a structural load. It is this last quality that makes cementitious materials so

T. Wangler (✉) · R. J. Flatt · L. Reiter
Institute for Building Materials, ETH Zurich, Stefano-Franscini-Platz 3, 8093 Zurich, Switzerland
e-mail: wangler@ifb.baug.ethz.ch

N. Roussel
Laboratoire NAVIER, Gustave Eiffel University, 5 Boulevard Descartes, 77420 Champs-sur-Marne, France

A. Perrot
University Bretagne-Sud, IRDL, UMR CNRS 6027, 56100 Lorient, France

M. Sonebi
School of Natural and Built Environment, Queen's University Belfast, Belfast BT9 5AG, Northern Ireland, UK

R. Wolfs · F. Bos
Department of the Built Environment, Eindhoven University of Technology, P.O. Box 513, NL-5600, MB Eindhoven, The Netherlands

D. Lowke · N. Freund
Institute of Building Materials, Concrete Construction and Fire Safety, Technische Universität Braunschweig, Beethovenstr. 52, 38106 Braunschweig, Germany

D. Stephan · U. Pott
Technische Universität Berlin, Department of Civil Engineering, Building Materials and Construction Chemistry, Gustav-Meyer-Allee 25, 13355 Berlin, Germany

N. Roussel and D. Lowke (eds.), *Digital Fabrication with Cement-Based Materials*,
RILEM State-of-the-Art Reports 36, https://doi.org/10.1007/978-3-030-90535-4_4

attractive for a wide variety of digital fabrication processes for construction, including extrusion-based 3D printing. These processes have been defined and classified in Chap. 2.

All fabrication processes with cementitious materials are governed by certain physical properties. Cementitious materials are classified rheologically as yield stress fluids, thus properties such as the yield stress and plastic viscosity have traditionally played a major role in conventional construction processes; especially in the prediction of flow during pumping and casting of conventionally vibrated and self-compacting concretes. In Chap. 3, however, the basic physics behind digital fabrication processes with cementitious materials have been identified and well developed, and while yield stress and viscosity play their expected major roles, other properties now take on a larger significance in the prediction of processing performance and success. These properties include the evolution of yield stress (commonly called "structural build-up", or sometimes "thixotropy") and elastic modulus. The yield stress evolution, in particular, has had some study in the context of self-compacting concrete casting and flow loss, but until now remains ill-characterised in terms of how the evolving microstructure leads to particular rheological behaviour. Thus, characterisation techniques for this property are a major portion of this chapter.

The goal in this chapter is to shortly distil the key properties identified from the basic physics given in Chap. 3, giving a short focus to the structural build-up. The traditional measurements for properties of interest are then shortly described, followed by a more detailed description of the newest measurement techniques that have been developed so far.

4.2 Process Rheological Requirements

4.2.1 Competing Stresses During Printing

In most printing processes in industry or academia, gravity-induced stresses inside the element being printed often dominate all other external sources of stresses (e.g. capillary driven stresses, vibrations, temperature fluctuations, to mention a few). Obviously, these stresses increase proportionally with the density of the material and

S. Grünewald
Delft University of Technology, Faculty of Civil Engineering and Geosciences, Concrete Structures Group, Stevinweg 1, 2628 CN Delft, The Netherlands

W. R. L. da Silva
Danish Technological Institute, Taastrup, Denmark

S. Grünewald · G. De Schutter
Ghent University, Department of Structural Engineering and Building Materials, Magnel-Vandepitte Laboratory, Technologiepark-Zwijnaarde 60, 9052 Ghent, Belgium

with length scale. This length scale may either be the thickness of the filament during the deposition stage or the height of the object already printed, which is therefore time-dependent (Roussel 2018; Mechtcherine et al. 2020). These stresses induce, in turn, some material deformation which can turn into flow if stress exceeds the material strength or cohesion (Roussel 2018; Mechtcherine et al. 2020). For some non-Newtonian-fluid-type printable materials, this strength or cohesion is called yield stress. It was, however, shown that, for some stiffer printable materials, this strength is very similar to the mechanical strength obtained and measured for brittle quasi-solid materials (Mettler et al. 2016).

Even if the conditions required for material flow onset and, therefore, printing instabilities are not reached, the "small" deformations induced by these gravity-driven stresses may be at the origin of non-acceptable deviations in the final object geometry. This is why, in addition to some strength requirements, there also exists requirements on the material rigidity or stiffness (Roussel 2018; Mechtcherine et al. 2020; Wolfs et al. 2018).

In other words, most printing processes success will be dictated by the result of a competition between gravity-induced stresses—that do scale with a local deposition thickness and/or object height—and some strength/cohesion/rigidity/stiffness material properties. If at any point through the entire printing process, gravity-driven stresses win the above competition, the process shall fail.

The exact terms used to describe the above strength/cohesion/rigidity/stiffness features of a given printable material vary among authors and printing processes but include e.g. **yield stress, cohesion, plasticity limit, friction angle, compressive strength, elastic modulus, critical strain, etc.** Most of these properties are expressed in Pa or kPa. Elasto-plastic models are often used to describe the material along with various plasticity criteria such as the Von Mises plasticity criterion and Tresca plasticity criterion, as well as the Mohr–Coulomb criterion in the case of frictional materials.

As these properties are often expected to change with time for cement-based materials for various chemical and physical reasons (see further in this chapter), material properties of interest also often include some kind of structuration/thixotropy rate (Roussel et al. 2019, 2012; Roussel 2005, 2006). These material properties, no matter their name or the way they are measured, capture the speed at which the strength/cohesion/rigidity/stiffness of the material being printed increases with time and are often expressed in Pa/s.

4.2.1.1 Printing Head Feeding

Before the printing phase dominated by gravity-induced stresses as described above, most processes in industry or academia involve some kind of material transport through a pipe. This transport typically occurs over a distance of several meters between a mixing device and a mobile printing or deposition head. Depending on the material consistency, pipe diameter and flow rate, these transport phases are either referred to as pumping or extrusion (Schutter and Feys 2016; Perrot et al. 2019). In

both cases, they involve a competition between a pressure applied to the material and its resistance to flow. The result of this competition drives the material flow rate in the pipe.

In the case of high flow rates, fluid materials and/or small pipes, the resistance to flow typically involves the material bulk viscosity if the material is fully sheared in the pipe or, most often, the viscosity of a so-called lubrication layer at the vicinity of the pipe wall. This lubrication layer is induced by the so-called "shear-induced particle migration" (Spangenberg et al. 2012; Choi et al. 2013) that pushes particles away from high shear rate zones. Shear rate concentrates in this lubrication layer depleted of coarse particles while the bulk material is almost unsheared, depending on its yield stress. In this case, the bulk material rheological behaviour matters less than the ability of the material to form a lubrication layer along with the layer's rheological properties.

In the case of low flow rates, stiff materials and/or large pipes, the above lubrication layer thickness possibly becomes of the order of the size of the smallest particles in the material. As a result, the concept of a lubrication layer displaying its own viscosity fails and the resistance to flow is often considered to find its origin into the frictional/tribological properties of the material (Perrot et al. 2019).

4.2.1.2 Filament Stability and Geometry Control

It is possible to go into more details when focusing on the deposition process. The length scale driving local gravity-induced stresses is obviously the thickness of the layers/filament/lace H_0. This thickness varying between 1.0 mm (for so-called "micro-printing") to around 10.0 cm for some large-scale industrial application, the resulting gravity-driven stress ($\rho.g.H_0$) shall be between around a couple of tens of Pa and a couple thousands of Pa. In order for the layer/filament/lace to be stable, the yield stress of the material, τ_0, being printed shall be in the same order of magnitude or higher, i.e. from 100 Pa to 10 kPa. The reader should note that this range of yield stresses is the same as the one covered by modern concretes, i.e. from 50 Pa for Self-Compacting Concretes to a few thousand Pa for traditional vibrated concretes (Yammine et al. 2008). We can expect that, at the stage of the deposition process, deformations greater than a couple % cannot be accepted. As a consequence, the minimum value of the elastic modulus of the material expressed as the ratio between the applied gravity-driven stress and the tolerable strain shall be between around 1.0 and 100 kPa.

4.2.2 Object Stability and Geometry Control

Through the printing process, the gravity-induced stress in a given layer increases with the number of layers printed above the considered layer. The competition between this gravity-induced stress that increases with time and the

strength/cohesion/rigidity/stiffness of the material being printed requires that the strength/cohesion/rigidity/stiffness of the material always stays higher. This requires, in turn, that either that the strength/cohesion/rigidity/stiffness (a) are, from the start, higher than the highest gravity-driven stress reached at the end of the printing process or (b) increase fast enough to always dominate gravity.

From a stress point of view, we can expect in the case of a slender vertical element that, for every meter in the vertical direction element of height, the strength/cohesion should increase by 20 kPa. The reader should note that this value is around the highest cohesion acceptable for a material that has to be pumped or extruded (see above). As a consequence, the above listed option (a) can only be applied to the printing of objects where the vertical dimension of which stays lower than 1.0 m.

In most cases, however, either the printing time is long (i.e. long printing perimeter) or the material is chemically or physically accelerated (see section further in this chapter). Hence, the increase of the material strength/cohesion in time has to be taken into account in the evaluation of the printing process and allows for higher vertical printed dimensions.

However, it was shown in a milestone paper (Wolfs et al. 2018) that, for high vertical dimensions, object stability is not driven anymore by the competition between gravity-induced stress and strength or cohesion but by the risk of so-called self-buckling or gravity-driven buckling. Such instability was shown to scale with the vertical dimension of the object at the power three (Roussel 2018). This imposes requirements not on strength/cohesion but primarily on the material rigidity/stiffness. These can reach levels as high as a few MPa for a 3.0 m high printed element. The reader should note that such levels of rigidity can only be reached through some kind of chemical reactions and not by the natural flocculation/structuration of cement-based products (see Sect. 4.3 further in this paper).

4.3 Background Chemistry and Chemical Admixtures

What has been termed structural build-up or yield stress evolution in cementitious materials is related to, primarily, two processes: the flocculation of particles, and the formation of hydration products. After a fluid cementitious material undergoes a shearing event (such as pumping and extrusion in digital fabrication), it is then placed, where it undergoes a period of rest and builds strength due to these two processes, which, despite occurring simultaneously, do occur to varying degrees and at different time scales. The areas where these two processes are primarily dominant are depicted in Fig. 4.1, with flocculation processes being dominant in the early stages up to a maximum, and then hydration processes dominating when these processes are initiated at the onset of the acceleration period. These processes their implications for digital fabrication with cementitious materials as well as a brief description of methods used to control them are described as follows. It should be stated, though, that the general relationship between microstructure and rheology and its evolution

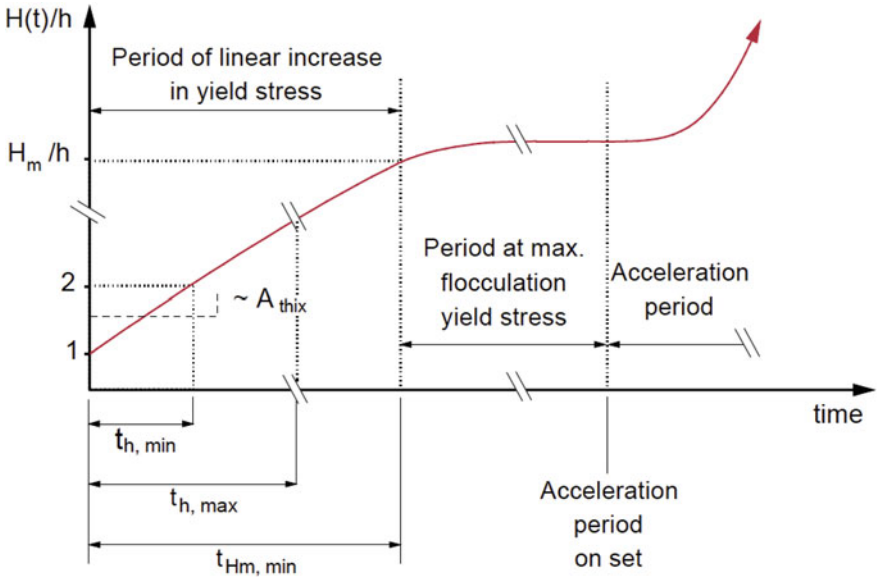

Fig. 4.1 Strength build-up (given in terms of height) over time for a cementitious material, schematically showing the period of the first linear increase due to flocculation before reaching a maximum, and then the exponential increase that occurs just after onset of the acceleration period. Figure adapted from Wangler et al. (2016), with variables fully described therein

is still a topic of intense research for cementitious materials, and it will remain so for the foreseeable future.

4.3.1 Flocculation (Thixotropy)

The term "Flocculation" is usually applied to processes that occur on short time scales during the dormant period of cementitious binders. Often these processes (time scales of seconds to minutes) are termed "thixotropic" processes (Roussel 2006; Roussel et al. 2012; Wallevik 2009; Assaad et al. 2003a, b).

The processes that generally govern interparticle forces when a colloidal suspension such as a cementitious binder is put at rest after a shearing event include: (1) Brownian, (2) colloidal, and (3) hydrodynamic forces. The colloidal forces, in particular, dominate the yield stress behavior of dense particle suspensions such as cementitious systems, varying in magnitude with interparticle separation. These forces can be either attractive (van der Waals) or repulsive (electrostatic or steric), with modifications to these interactions possible through the use of adsorbent molecules such as superplasticizers (Yang et al. 1997; Gelardi and Flatt 2016). Besides these forces, suspension characteristics such as solid volume fraction (related

to the w/c ratio) along with particle size and distribution play a large role (Zhou et al. 1999; Flatt and Bowen 2006).

During the period dominated by flocculation processes, however, low-level hydration is also occurring, which contributes to structural build-up through the formation of solid bridges between particles (Roussel et al. 2012) or the formation of additional surface area for consumption of superplasticizer from solution (Mantellato et al. 2019).

4.3.2 Hydration

Cementitious systems are unique for colloidal suspensions in the sense that they are reactive. Hydration processes, related to the dissolution of aluminate (C_3A) and silicate (C_3S, C_2S) clinker mineral phases and the subsequent nucleation and growth of new phases (hydrates), begin immediately upon the first contact with water. These processes vary over time and magnitude for the different mineral phases, with different consequences for the overall rheological behaviour of the suspension. This chemical activity evolves heat, which can be measured in a calorimetry experiment (Sect. 4.5) A typical heat evolution curve for a cementitious material is depicted in Fig. 4.2.

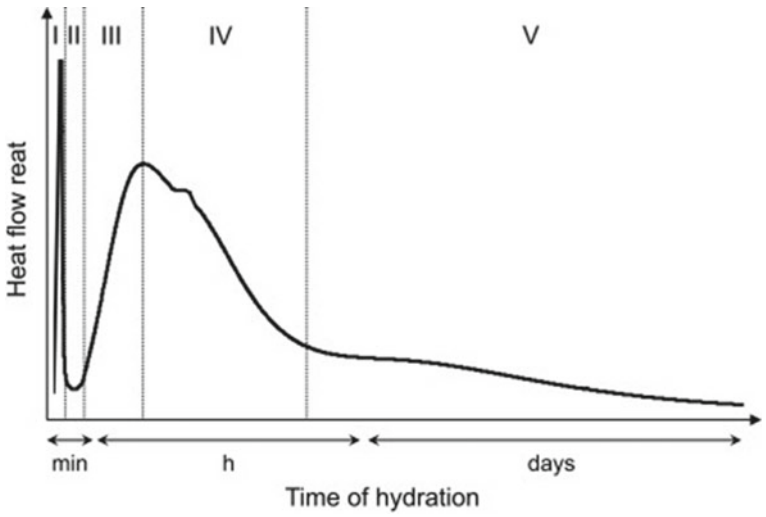

Fig. 4.2 Typical hydration heat curve for a cementitious material, showing 5 distinct stages. Of greatest interest for digital fabrication processes are stages I and II, until the onset of the acceleration period, which occurs when stage II transitions to stage III. Figure from Marchon and Flatt (2016)

The hydration curve is characterised by stages noted in Fig. 4.2:

- Stage I: dissolution of sulfate and highly reactive C_3A phases, happening rapidly within the first minutes of water contact.
- Stage II: dormant period or induction period, with low chemical activity and characterised by having a workable paste, generally lasting on the order of one to two hours (also known as the "open time").
- Stage III: acceleration period, where paste loses its workability (setting) and C_3S hydration dominates (formation of primary strength-giving phase, calcium silicate hydrate, C-S–H), generally lasting for some hours.
- Stages IV and V: deceleration period, where diffusion controlled growth dominates, lasting for days to months.

For the purposes of digital fabrication processes, Stage I and II are of primary interest, when concrete must remain fluid (and processable) up to placement. These correspond to the period of time where both flocculation and local hydration processes are dominant (Roussel 2012). The Stage II transitions to Stage III is termed the "onset" of acceleration. The massive generation of hydration products increases yield stress in cementitious materials because of the formation of new surface area, which consumes superplasticizer and increases contact points between cement grains, and ultimately the formation and strengthening of C-S–H bridges between cementitious particles.

4.3.3 Chemical Admixture Control—Set-On-Demand

As described in detail in Chap. 3 and reminded shortly in Sect. 4.3.1, the rheological requirements of cementitious materials within a given digital fabrication process can vary widely. Rheological changes from a more fluid, low yield stress and pumpable material, to a stiff, high yield stress material sometimes must occur within a matter of seconds. More critically, the buildability of the material requires that yield stress increases linearly over time to match the build rate, or depending on component geometry, that the elastic modulus of the material increases exponentially (Wolfs et al. 2018; Roussel 2018; Reiter et al. 2018). The maximum yield stress increase of cementitious materials in the dormant period is limited (Wangler et al. 2016), thus the use of chemical admixtures that are very strongly flocculating or that actually induce or enhance the formation of hydration products are strongly advised.

A review of the chemical admixtures used in digital fabrication processes has recently been published (Marchon et al. 2018), and the primary types are summarised as follows:

- **Superplasticizers**: these admixtures reduce yield stress and viscosity at constant solids content, which makes them natural choices for the initial rheological requirements of flowable concretes, helping mixes to reach a proper pumpability. In certain digitally controlled casting processes such as Smart Dynamic Casting,

they are essential not just in the pumping process but also the placement process. The most widespread type of these admixtures are the polycarboxylate ethers (PCEs), which are comb copolymers consisting of an anionic backbone which adsorb to the cement particles, and uncharged side chains that extend into the solution and prevent particle contact through steric hindrance.

- **Viscosity modifying agents (VMAs)**: these admixtures are generally long-chain organic molecules that increase suspension viscosity by bridging and binding across particles. They also tend to increase the yield stress through this mechanism, and it is in this that they have found utility in digital fabrication processes, by imparting a sometimes rather high initial yield stress, as well as by increasing buildability through increasing thixotropy.
- **Retarders**: these admixtures generally consist of sugars and other carbohydrates, with sucrose being one of the most powerful. They control the open time of a given batch of cementitious material, allowing it to remain workable and processable for extended periods of time.
- **Accelerators**: accelerators are a class of admixture that accelerate the formation of hydration products, which as described earlier, is the most useful mechanism for building strength quickly in digital fabrication systems. Accelerators typically can act on the silicate phases, accelerating the formation of C-S–H (the primary strength-giving phase in cementitious materials) through either the addition of calcium ions (in calcium salt formulations) or the addition of C-S–H seeds to seed nucleation (Thomas et al. 2009; Myrdal 2007). Recent results have suggested that this pathway to strength build-up may be too slow for targeted vertical build speeds of some digital fabrication processes, and thus the accelerators that target the formation of aluminate phases, especially ettringite, have been the focus of research. These accelerators are already being used successfully for many years in shotcrete processes, and generally consist of aluminium salts which promote the fast precipitation of ettringite. More recently, the use of mineral substitutions of phases high in calcium, aluminium, and sometimes sulfate (in calcium aluminate cement or calcium aluminosulfate cement) has been explored and in some cases successfully implemented in digital fabrication processes (Khalil et al. 2017; Reiter et al. 2020), and further development of these chemical processing systems remains a major interest as the field develops.

The identification of the suitability of chemical admixtures for a digital fabrication process is simply the first step, however. Their successful implementation in a digital fabrication process involves precision in when and where to add them in the process. Reiter et al. (2018) pointed out that acceleration should take place as close as possible to the point of placement to avoid hardening in the processing lines, and with some of the fast-acting accelerators described above, this is absolutely essential. The development of inline or secondary mixing steps, in which an accelerator is added just before placement, has been described in Chap. 3 and is depicted in Fig. 4.3 below from Reiter et al. (2020). This concept shows a combination of retarded concrete to which an activator is added just before placement. Other systems have been developed

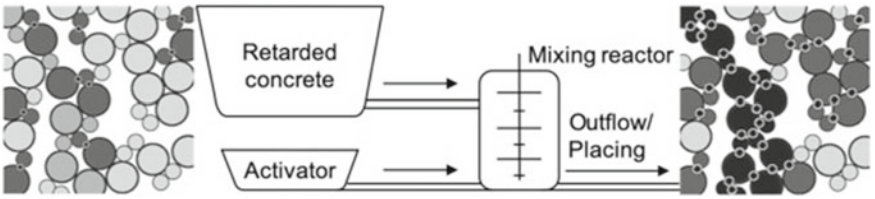

Fig. 4.3 Concept for processing of concrete in a Set on Demand system. A retarded concrete batch is pumped to a mixing reactor, where an activator is mixed in just before outflow and placement. Such a system enables well-timed control of material rheology, enabling proper structural build-up for process success. Figure from Reiter et al. (2020)

in which material is continuously mixed upstream, giving adequate open time in the line to avoid retardation before the inline mixing step.

4.4 Measurement Methods

4.4.1 Existing Measurement Methods

4.4.1.1 Free Flow

Free flow of cement-based materials is understood to be the flow of the material under its own weight. In most conventional construction site, rheology of fresh concrete is evaluated every day using gravity thanks to the Abrams cone (Roussel 2011). This standardised procedure is used as quality control test to ensure that the concrete has proper workability or so called "consistency" in order to fill formworks. However, the Abrams cone has been shown to be able to provide rheological parameters when using adequate assumption on the flow geometry (Bouvet et al. 2010; Pierre et al. 2013; Roussel and Coussot 2005; Ferraris and Larrard 1998). Such measurements have been considered to be fast and simple to carry out, and the Abrams cone has been called the "fifty-cent rheometer" (Roussel and Coussot 2005; Pashias et al. 1996). The slump test is used more often as a means of rapid and continuous checking to ensure uniformity of fresh concrete production or supply, rather than solely as a test for the assessment of workability. In all cases, the analysis is based on the description of the flow stoppage when the material yield stress balances the gravity-induced stresses.

For stiff concrete, when the slump is lower than the initial height of the cone, the flow can be considered as purely elongational, and the yield stress can be easily computed from the final height of the tested sample (Roussel and Coussot 2005; Pashias et al. 1996). On the other hand, for fluid concrete such as self-compacting mixtures, purely sheared flow is generated in a thin layer. In this case, the yield stress can be computed from the diameter of the spread flow (Bouvet et al. 2010; Roussel and Coussot 2005). Between those two extreme cases, a combination of these types

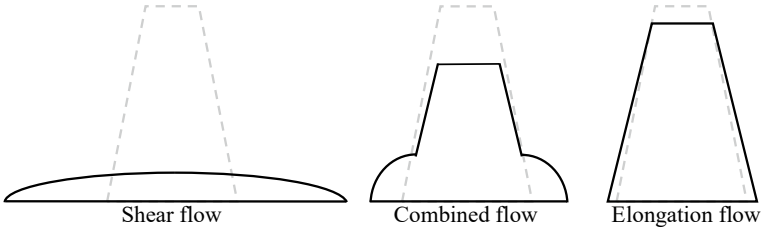

Fig. 4.4 Different scenarios of gravity-induced flow of a cementitious material cone (Dotted line: initial shape—Black line: final shape)

of flow occurs, and several studies have provided a relationship between the material yield stress and slump (Bouvet et al. 2010; Pierre et al. 2013). These three cases are illustrated in Fig. 4.4.

It can be noted that the cone geometry can be downscaled to the mortar scale (Bouvet et al. 2010) and that viscosity can also be estimated when performing the spread flow. The relationship linking the time to reach a spread diameter to the material plastic velocity is reported by Drewniok et al. (2017). Recently, The Danish Technology Institute has developed a version of the slump flow with further rheological parameter estimation based on the image analysis recorded by a camera during testing (Thrane et al. 2007, 2009).

Other geometries have been used to evaluate the rheological behaviour using gravity as the motor of the flow, especially with fluid concrete. Among those geometries, the L-Box, the LCPC-box can be used to determine the material yield stress (Nguyen et al. 2006; Roussel 2007; Thrane et al. 2004; Nielsson and Wallevik 2003) from the free surface obtained at the low stoppage and the V-funnel and the Marsh cone can be used to determine the viscosity from the time when mortar or concrete flow out from Marsh cone or V-funnel (Utsi et al. 2003; Le Roy and Roussel 2005; Roussel and Le Roy 2005). Those geometries can be seen in Fig. 4.5.

4.4.1.2 Rotational Flow

Generalities on Rotational Rheometry

Rotational rheometry can be considered as the conventional way to characterise the rheological behaviour of fluid materials and equipped commercially available rheometers. Conventional rheometers can be used for cement pastes and fine sand mortars and robust and specially dedicated rheometers have been designed for concrete (Koehler et al. 2005; koehler and Fowler 2004; Wallevik 2008, 2015; De Larrard et al. 1996; Hu et al. 1996).

Among others, three types of geometry have been used to measure the rheological properties of materials: coaxial cylinders, parallel plate geometry and cone plate geometry. Cone plate geometry is not often used in case of cementitious materials

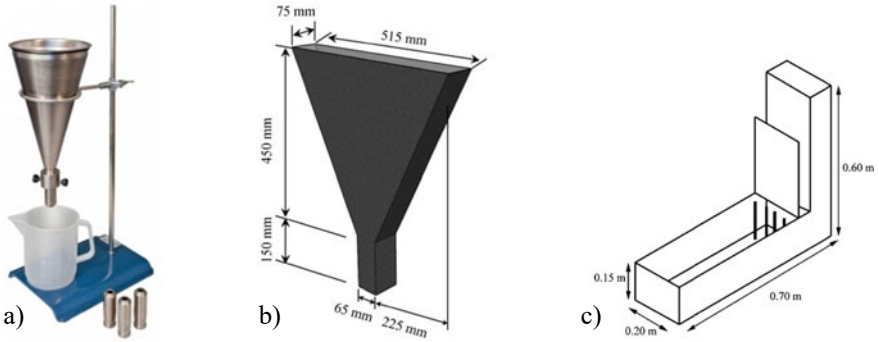

Fig. 4.5 Different types of geometries for rheological characterisation of cementitious materials using gravity-induced flow: **a** Marsh cone; **b** V-funnel (Ma and Wang 2018); **c** L-Box (Nguyen et al. 2006). Note that the LCPC-box is just the straight horizontal canal of the L-box

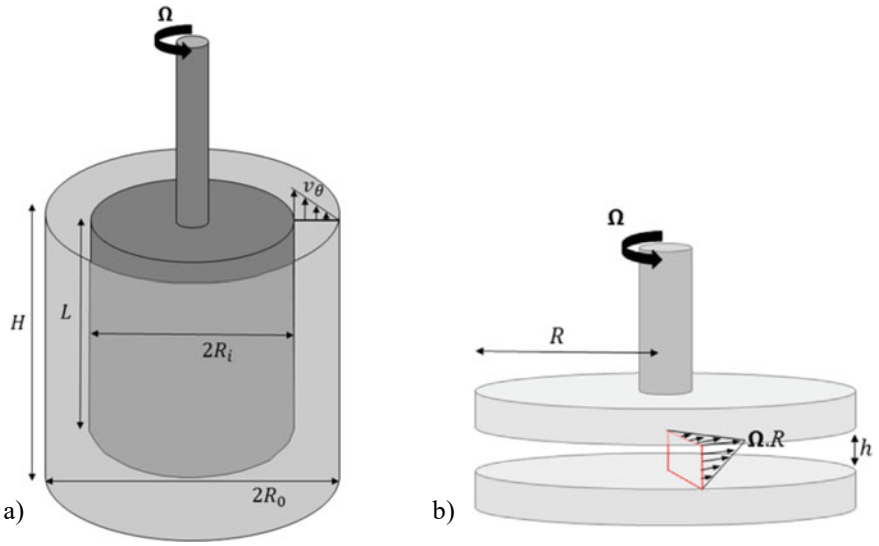

Fig. 4.6 Schematic of conventional rotational geometries. **a** Coaxial cylinders; **b** Parallel plates. Reproduced from Feys et al. (2018)

because of the size of the particles that are not adapted to the gap size at the center of the sample. Parallel plates and coaxial cylinders are depictured in Fig. 4.6.

In comparison to other materials such as polymers, one major issue when testing cementitious materials is linked to slippage. In order to solve this problem, a rough surface can be used to prevent slippage, and special tool such as 4 or 6-bladed vane or helicoidal tool that describes a cylinder during their rotation can be used as the inner cylinder in the coaxial geometry (Wallevik 2003, 2008; Barnes and Nguyen 2001; Estelle and Lanos 2012).

In all geometries, the tested material is confined between two surfaces (gap), one surface being fixed and the other can be submitted to a rotational movement in order to induce a shear flow. The basic principles of the test consist in imposing a rotational velocity to the rotating tool and to measure the resisting torque (controlled shear rate—CSR—mode) or in imposing a torque and measuring the resulting rotational velocity (controlled shear stress—CSS—mode).

Depending on the imposed solicitation, it is possible to measure shear static yield stress (Mahaut et al. 2008; Perrot et al. 2012), structural build-up (Tchamba et al. 2008; Ma et al. 2018; Lecompte and Perrot 2017), the entire material flow-curve at steady state (Feys et al. 2012; Estelle et al. 2008) or the viscoelastic properties of the studied materials (Mostafa and Yahia 2016; Schultz and Struble 1993).

Yield Stress Determination

For each geometry, the measurement of the static yield stress (i.e. the yield stress after a given resting time) can be measured using different test procedure including stress growth (CSR mode) (Mahaut et al. 2008; Perrot et al. 2012), stress ramp (CSS mode) (Banfill and Kitching 1990) or also creep recovery (CSS mode) (Feys et al. 2018; Qian and Kawashima 2016; Yuan et al. 2017). For the stress growth, plotting the recorded stress versus the strain can also help to describe the behaviour before the flow onset and can be used to compute a shear elastic modulus (Roussel et al. 2010). Repeating the test procedure after different resting time makes it also possible to compute the structural build-up rate A_{thix} of the tested cementitious material (Roussel 2006).

Identifying the Parameters of the Rheological Behaviour

Using strain rate ramp (CSR mode), it is possible to describe the steady-state rheological behaviour over a range of several orders of magnitude of strain rates using coaxial geometry (Koehler et al. 2005; Estellé and Lanos 2012) or parallel plate geometry (Wallevik 2015, 2016). The aim of such procedure is to obtain the parameter of steady-state rheological behaviour such as dynamic yield stress and plastic viscosity for the Bingham model and also the flow index for the Herschel-Bulkley model (Feys et al. 2012; Estellé et al. 2008). Different methods of data processing can be found in the literature. In coaxial geometry, the most used method is based on the Reiner-Riwlin equation that takes into account the possibility of an unsheared zone within the gap due to the material yield stress (Feys et al. 2012, 2018).

It has been pointed out that the data should be carefully analysed using an adequate choice of the model; otherwise non-physical negative yield stress value can be found (Feys et al. 2018; Wallevik et al. 2015). Also, care must be taken to the material homogeneity during the measurement (Feys et al. 2018; Wallevik et al. 2015): the strain rate field within the gap is very heterogeneous for the parallel plates and the coaxial geometry promoting shear-induced particle migration (Spangenberg et al.

2012). Also, flow curves are difficult to obtain for dilatant high yield stress material, because of failure localisation at the rotating tool surface at the flow onset. In this case, once the sample is broken, space is remaining between the rotating tool and the sample because gravity is not sufficient to make the material flowing and filling this space (Pierre et al. 2016).

Oscillatory Rheometry

Oscillatory rheometry has been used on cement pastes and mortars in order to follow the evolution of the viscoelastic properties of the cementitious material at rest (Feys et al. 2018; Ma et al. 2018; Schultz and Struble 1993). Such measurement can be used with coaxial, cone plate or parallel plate geometry. The basic principles of this kind of test called "Small Amplitude Oscillatory Shear" is to impose an oscillatory strain solicitation with an amplitude below the critical strain of the tested material (around 10^{-4} for a cement paste at rest) at low frequency (around 1.0 Hz) (Feys et al. 2018; Ma et al. 2018; Mostafa and Yahia 2016; Yuan et al. 2017). The imposed oscillatory strain is sinusoidal and can be written as follows:

$$\gamma(t) = \gamma_0 \sin \omega t \tag{4.1}$$

With γ_0 the strain amplitude and ω the oscillatory frequency. The stress response of the material can be written in the following form (Schultz and Struble 1993):

$$\tau(t) = \gamma_0 (G' \sin \omega t + G'' \cos \omega t) \tag{4.2}$$

With *G'* the shear storage modulus and *G"* the shear loss modulus. The storage modulus *G'* describes the in-phase elastic solid-like component of the material behaviour while *G"*, the loss modulus, represents the viscous out-of-phase component of the behaviour.

At low shear strain, the viscous effect can be neglected in comparison with elastic effect, which means that the stress response is almost in phase with the strain solicitation and, therefore, that the apparent elastic modulus can be approximated by the storage modulus (Roussel 2018; Roussel et al. 2010). Assuming a constant critical shear strain and a linear elastic behaviour, the yield stress, τ_c, can be computed from the storage modulus $\tau_c = G'.\gamma_c$. Consequently, the monitoring of the storage modulus can be used to study the material structural build-up as performed in several studies.

This continuous measurement of the structural build-up may stop when the torque capacity of the rheometer is exceeded or when the becoming rigid material starts to slip at the interface.

4.4.1.3 Confined Flow

For high yield stress cement-based materials, free flows and rotational flows are not suitable for determining the viscous component (i.e. after the flow onset) of the material behavior because gravity forces are too low and because of shear localisation (Pierre et al. 2016).

In order to assess the viscosity and the steady-state flow curve of such firm mixtures, confined flows can be used and studied in order to both generate sufficient stresses to both make the material flowing and avoid the generation of some localised fractured shear surfaces. Different geometries can be used to generate confined flows: squeeze flow (Roussel and Lanos 2003; Engmann et al 2005; Toutou et al. 2005), back extrusion (Perrot et al. 2011) or ram extrusion (Zhou and Li 2005; Perrot et al. 2012; Zhou et al. 2013).

Squeeze flow is used to describe the rheological behaviour of firm concentrated suspensions such as molten polymers, food materials or ceramic pastes (Roussel and Lanos 2003; Engmann et al. 2005; Chan and Baird 2002). The test consists of a simple compression test on a cylindrical sample placed between two coaxial and circular plates. The compression of the sample of radius, R, height, h, and at a constant velocity, v, induces an elongational flow. The radii of the sample and the plates can be the same or not. In the first case, the volume of the sample remains the same during the test (sample diameter lower than plates diameter), and in the second, the surface between the sample and the test remains constant (sample diameter equal to the plate diameter). In any case, it is important to use a rough surface to avoid material slippage at the plates interface (Roussel and Lanos 2003). Analytical model of the squeeze flow of Bingham or Herschel-Bulkley fluids are available in the literature (Engmann et al. 2005).

Axisymmetric ram extrusion flows are used to estimate the flow properties of so-called "zero-slump" mortars for which rotational rheometers are not applicable (Zhou and Li 2005; Perrot et al. 2012; Zhou et al. 2013; Mimoune and Aouadja 2004; Alfani and Guerrini 2005; Alfani et al. 2007). The methods and techniques used for cement-based materials are inspired by the literature on ceramics, especially the works of Benbow and Bridgwater (Benbow and Bridgwater 1993; Händle 2007). The material located inside the extruder barrel is pushed by a ram towards a circular die that gives its final shape to the material. The required force that allows to overcome the shaping force required to give its final shape to the material in the shaping zone denoted F_{pl} and the wall friction force, F_{fr}, developed along the extruder barrel is linked to the interfacial stress.

The shaping force is used to study the bulk rheology of the material using the methodology proposed by Perrot et al. (2012) or Zhou et al. (2013). Contrary to rotational rheometry, several tests are needed to describe the whole flow curve of a cement-based material, because one extrusion test carried out at a constant ram speed is representative of a single average shear rate. This means that an extrusion test provides only one point of the flow curves. The friction force is used to measure the tribological behaviour (interfacial rheology) of the cement-based materials.

Axisymmetric back extrusion is used to generate an upward flow in the gap between the plunger and the container. The induced shear flow can be used to determine the rheological behaviour of firm cement-based material (Perrot et al. 2011).

For those confined geometries, a problem of water filtration may appear, leading to a heterogeneous mortar (Perrot et al. 2014, 2019). Such filtration is likely to appear for low-velocity test or for mortar or cementitious material which do not contain fine powder or viscosity modifying admixtures and, therefore, exhibit a high permeability (Perrot et al. 2014). When filtration appears, the recorded force increases, and the above described techniques cannot be used to reliably measure the rheological behavior of studied material.

4.4.1.4 Limitations for 3D Printing Formulations

From the above section on conventional rheological methods, it can be seen that there is no experimental method that is optimised for the online monitoring of the rheological behaviour of the cementitious material during printing.

Such an idealistic method should be simple, robust and be able to describe the full range of rheological behaviour from fresh fluid to early setting solid material. Free flow is not suitable for high yield stress material or high thixotropy material. For rotational rheometry, oscillatory shear is interesting but requires an expensive device and is limited by the torque capacity of the rheometer. Also, confined flows are destructive methods that cannot be used to follow the structural build-up of the materials.

Therefore, it is required to develop new types of rheological tests that are process-related and able to assess the evolution of the required parameter of the material behaviour.

4.4.2 Methods Utilised or Developed for Digital Fabrication with Concrete

Test methods typically adopted to assess the properties of fresh concrete before setting target the material in a fluid state, as discussed in Sect. 4.4.1, with well-known and robust methods established to measure both yield stress and viscosity. While these properties are of great importance to control the processing phases in digital fabrication, (e.g. pumping and extruding), the properties in the subsequent static state of fresh concrete should be addressed as well, in particular, their evolution in time. Due to the absence of confinement by traditional formwork, which characterises the majority of digital fabrication processes, the mechanical properties of fresh concrete and their development in time, or structuration rate, are of vital importance to control the structural behaviour during the fabrication process and prevent collapse. As the

relatively high initial strength and stiffness, or rigidity, of material compositions often adopted prevent correct measurements by traditional rheological tests, or because the nature of these test simply does not provide the appropriate parameters, various mechanical tests have been adopted instead. These are outlined in the following sections.

In contrast to traditional construction practice, concrete is typically not compacted in a digital fabrication process. It was shown that an overestimation in material properties may occur when material is extracted and compacted before testing, for instance to remove the presence of layer interfaces in samples created by a 3D printing process (Wolfs et al. 2019), as this affects the presence of e.g. voids or (micro)-cracks after extrusion. As such, regardless the adopted test, it is essential that the fresh concrete is tested in a state and scale representable of the digital fabrication process. Besides, due to the sample state and size, it is generally not possible to apply physical measurement devices without initiating unintentional thixotropic breakdown. Such a device may, moreover, restrict and influence the (natural) deformation behaviour of the fresh material, which generally exhibits relatively large deformations. It was successfully shown that optic measurement techniques may be adopted instead (Wolfs et al. 2018). Finally, in comparison to mechanical testing of hardened concrete, tests on fresh material should be executed swiftly to eliminate the influence of ongoing hydration and flocculation within a single test and to be able to attribute the properties to a specific age (Mettler et al. 2016; Wolfs et al. 2018).

The result of these challenges has led to a number of researchers developing a variety of methods to measure these properties, with some measurements able to measure more than one property. These measurements are detailed in the following.

4.4.2.1 Compression

Compression tests may be performed on fresh concrete to derive the compressive strength, Young's modulus, and Poisson's ratio, as well as their development as a function of concrete age. Based on ASTM D2166, these tests are typically performed on cylindrical samples with a height-to-diameter ratio between 2.0 and 2.5, whereby the largest particle size is smaller than one-sixth of the specimen diameter. The cylinders are vertically compressed by a loading plate, and the corresponding vertical and lateral deformation is recorded. The resulting load–displacement relation may be translated into stress–strain diagrams to derive the desired material properties. The unconfined compressive strength is defined for each test as the maximum occurring stress, and the Young's modulus and Poisson's ratio are derived within the linear range of the stress–strain relation. A compression test does not allow for testing of multi-axial stress states. In various studies, the compressive strength and stiffness were found to increase significantly as the material ages, and their evolution may follow both a linear (Roussel 2006) and non-linear trend (Lecompte and Perrot 2017).

In a time span of a typical digital fabrication process with concrete, i.e. several minutes to a couple of hours, a transition of plastic towards brittle failure may be observed. For instance, in Fig. 4.7, the failure modes of compressed specimens are

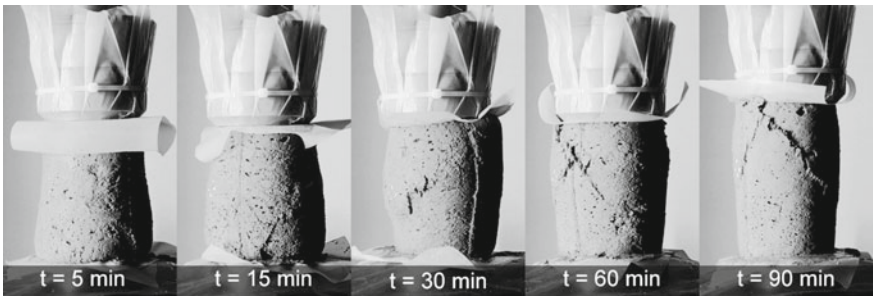

Fig. 4.7 Failure modes as observed in the compression test on fresh 3D printed concrete. Reproduced from Wolfs et al. (2018)

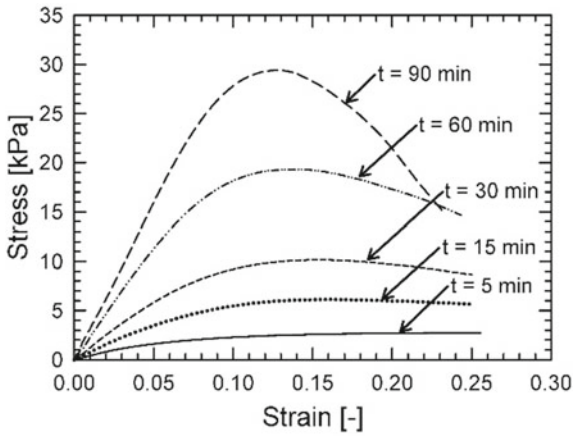

Fig. 4.8 Stress–strain relation of 3D printed concrete tested by compression at various ages, depicted in Fig. 4.7. Reproduced from Wolfs et al. (2018)

depicted for 3D printed concrete at various ages of 5 to 90 min after extrusion. Due to the relatively low stiffness, the early age specimens significantly expand in lateral direction as the vertical deformation increases, and fail by plastic 'barrelling' (bulging). In contrast, older specimens expand less in the lateral direction, and show a distinct and brittle failure plane formation. The intermediate samples show an intermediate failure behaviour. This transition of failure modes was likewise observed in similar studies targeting the material properties of fresh concrete in the context of digital fabrication (Mettler et al. 2016; Wolfs et al. 2019).

4.4.2.2 Shear

Shear tests may be performed on fresh concrete to define a failure criterion and its evolution as the material ages. A variety of shear tests is available (see e.g. ASTM D2166, or D6128), but in essence, they are all based on the horizontal displacement of a two-part, often cylindrical, specimen, see Fig. 4.9. One part is kept stationary,

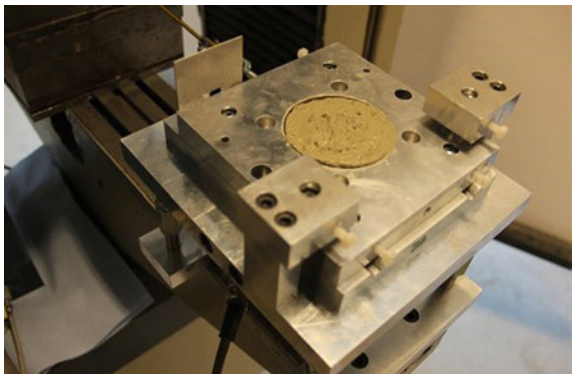

Fig. 4.9 Close up of a direct shear test on 3D printed concrete, without a normal force applied. Reproduced from Wolfs et al. (2018)

while the other is horizontally displaced by an external load. In vertical direction, a constant normal force may be applied to the specimen prior to shearing. The resulting maximal shear force may be used to derive the specimen shear strength. Due to the non-uniform stress and strain distribution during shearing, this test is not suitable to derive stiffness properties.

By deriving the shear strength for various vertical forces applied, a failure criterion can be constructed. It was shown that, for certain 3D printable mixture compositions, the Mohr–Coulomb theory may provide a satisfactory failure criterion (Wolfs et al. 2018; Jayathilakage et al. 2019), as the increment in normal force resulted in higher shear strength. This criterion is based on two material parameters, the cohesion and angle of internal friction, which are easily derived by performing a series of shear tests with various normal forces. Similar to the properties derived by the compression test, see Sect. 4.4.2.1, the cohesion and angle of internal friction were found to increase during the time span of a typical digital manufacturing process in recent studies (Mettler et al. 2016; Wolfs et al. 2018), indicating a transition from a fluid material towards a solid.

A well-known issue in shear tests is the friction between the two halves of the test setup, reported by e.g. Assaad et al. (2014, Liu et al. (2005). In particular, for (very) early-age concrete, the resulting friction force may contribute significantly to the total shear force and compromise the accuracy of the test. This issue may be addressed by treating the setup prior to testing, for instance, by machine-milling grooves in the two halves of the setup and applying rollers in between (Wolfs et al. 2018).

4.4.2.3 Triaxial Compression

A triaxial compression test may be adopted to derive both the stiffness properties and those needed to define a failure criterion for fresh concrete. As such, it can provide all required properties needed to assess both failure by elastic buckling and plastic collapse. Based on ASTM D2850, in a triaxial test a specimen is subjected

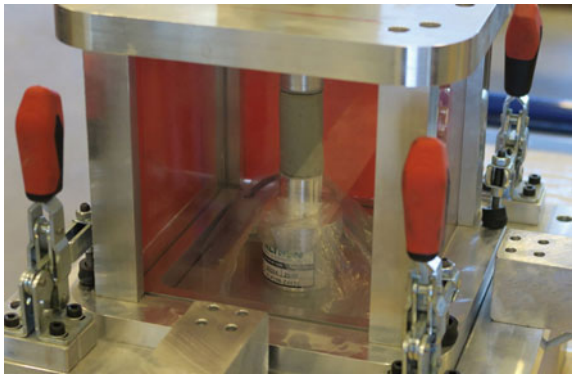

Fig. 4.10 Close up of a triaxial compression test on 3D printed concrete. Reproduced from Wolfs et al. (2019)

to a constant confining pressure and is then compressed in vertical direction until failure. Similar to the compression test, triaxial tests are performed on cylindrical samples with a height-to-diameter ratio between 2.0 and 2.5, such that a shear failure plane may be induced. The confining pressure may be applied via e.g. water, oil or air, and as such, the specimens are tested in a closed chamber, see for instance Fig. 4.10. In contrast to triaxial tests on hardened matter (e.g. soil, rock, concrete), the specimen deformation cannot be measured directly on the sample, which may be overcome by designing the triaxial chamber in cubic shape, such that optic deformation measurements may be applied instead.

By recording the specimen deformation and vertical force for various confining pressures, a failure criterion may be derived, such as the Mohr–Coulomb criterion that was found to be suitable for fresh concrete in the time span of a typical 3D printing process (Wolfs et al. 2019). A triaxial test with no confining pressure applied may be considered as uniaxial compression test, and as such, provides the stiffness and deformation parameters of the fresh material.

The deformation measurements of the triaxial test may be additionally applied to derive the dilatancy behaviour of fresh concrete, which indicates the change in volume associated with (plastic) shear distortion of the material. However, since plastic deformation during a digital fabrication process may already be considered as failure, the dilation behaviour is of lesser importance for the majority of studies targeting fresh concrete in this context.

4.4.2.4 Tension

A tensile test may be performed on fresh concrete to define the early age tensile strength and its development. The test may be performed using a mould of two separable parts, of which one part is horizontally separated from its fixed counterpart, see Fig. 4.11. The tensile force required to induce sample failure may be used to define the specimen tensile strength.

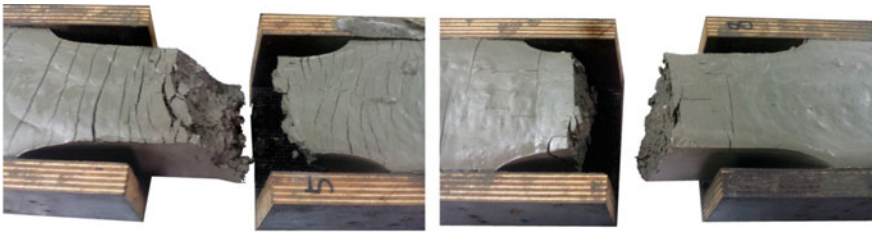

Fig. 4.11 Close up specimens of fresh concrete in a tensile test. Reproduced from Mettler et al. (2016)

Contrary to the tensile test on hardened specimens, fresh concrete cannot be clamped. An internal pin structure may be attached to the box walls, to enhance shear force transmission from the mould to the sample (Mettler et al. 2016). By applying a round notch to the specimen, controlled failure at the specimen center may be induced without introducing peak stresses.

4.4.2.5 Ultrasound

The measurement of ultrasonic pulse velocity in cementitious materials has been used by some groups for monitoring strength build-up of cementitious materials in digital fabrication technologies (Wolfs et al. 2018; Chen et al. 2019), and it has anyway been used historically to monitor setting times and strength build-up in cementitious material systems in general (Lee et al. 2004; Reinhardt et al. 2000; Trtnik et al. 2008). The physical principle is based on the measurement of the speed of sound in a sample; a transducer emits a signal which is received by another transducer or reflected back to the original transducer. The time delay and distance travelled between emission and reception gives a velocity. This velocity is proportional to the shear modulus of the material, which is then assumed to be proportional to the yield stress. It should be noted that because this method is nondestructive, a critical deformation must be assumed in order to estimate the yield stress, and this critical deformation is not necessarily constant with the material evolution. Therefore, as it was performed in the study of Wolfs et al. (2018), ultrasonic pulse velocity measurements to determine the strength evolution over time is only useful if empirically correlated with strength measurements.

4.4.2.6 Penetration

The methods described until now for measuring yield stress, while having many advantages, often have disadvantages such as that of requiring extensive sample preparation, large sample sizes, or being pointwise measurements requiring multiple samples, as in the compressive, tensile, triaxial strength measurements, to mention

a few. Certain methods can also have the limitation of not being destructive, which requires then an estimation of the critical deformation, which is not necessarily constant over time. Even destructive measurements, which actually do deform the material until the onset of flow can have the limitation of having a shearing surface at the interface of the material with the instrument, rather than within the bulk of the material, such as in vane rheometry experiments. The ideal method thus would have the advantages of being a continuous measurement on a single sample, with the shear surface within the bulk of the sample. Penetration tests can offer such advantages, if designed appropriately.

Penetration tests have been used historically with cementitious materials to measure setting times of pastes and mortars (ASTM C191 and ASTM C403) and have also been used to measure the penetration resistance of soils (ASTM D3441 and D1558). The tests on cementitious materials can be called "fast" penetration tests, as they are performed pointwise, and the soil penetration resistance tests can be called "slow" penetration tests, as they measure penetration force with time at a slower displacement rate, and it can happen over a time interval of interest with a single measurement. A more recent European Norm (EN 14,488–2) describes the use of penetration tests to determine the compressive strength of young sprayed concretes by shooting or pressing a penetration tip into the material, another "fast" penetration test.

As the penetration force is primarily influenced by the yield stress of the material, one can consider the penetration test to be a rheological measurement. A 2009 paper by Lootens et al. (2009) examined the use of these penetration tests in the assessment of yield stress of setting cement pastes. The authors found a very strong correlation of these tests with the yield stress, and they developed analytical relations between the test type, needle and tip geometry, and the respective yield stress or compressive strength. Generally speaking, the test should be performed in a controlled manner in material undisturbed by previous testing. The penetration force is expected to scale with the shearing surface, which is expected to be proportional to the penetration tip surface in contact with the material, as depicted in Fig. 4.12.

As these tests are of great relevance in the region of interest for cementitious materials used in digital fabrication, some researchers have examined their use in the context of digital fabrication, which is detailed in the following.

Fast Penetration

Within the Shotcrete 3D Printing process (SC3DP) (Kloft et al. 2020; Dressler et al. 2020) both process-related (e.g. pumping and spraying) and material-related factors (e.g. set-accelerator dosage) have a significant effect on the resulting yield stress evolution. In order to investigate these influencing factors systematically within the printing process, an in situ yield stress measurement on printed test specimens is indispensable. For this purpose, a shotcrete penetrometer (Mecmesin Shotcrete Penetrometer) with a defined needle geometry (diameter: 3.0 mm, cylindrical height: 12.5 mm, cone height: 2.5 mm) has been used (Dressler et al. 2020)—the

measurement has been performed manually. This penetrometer is designed and used based on EN 14,488–2. The penetration depth is set at 15.0 mm, Fig. 4.13 (left). A repetition of 5–10 measurements is recommended in order to obtain a statistical certainty. Depending on the research objective, measurements can be performed at any time interval. According to the study by Lootens et al. (2009), the penetration resistance can be calculated to a yield stress. Figure 4.13 (right) shows exemplary results obtained on the basis of fast penetration tests. It shows the effect of different set accelerator dosages on the yield stress evolution of Shotcrete 3D printed samples.

In the same fashion, Lloret et al. (2015) used fast penetration tests to assess the structural build-up of a self-compacting mortar in Smart Dynamic Casting, a digitally controlled slipforming process. They empirically correlated penetration force to slipping speed to determine a material processing window. The previously cited study of Mettler et al. (2016) went further with this method to correlate the penetration load to yield stress of the self-compacting mortar, as well as to detail its transition from the liquid to the solid state. They used a penetration tip of a disc with a diameter of approx. 19.0 mm mounted on a triaxial table and driven at a speed on the order of 1.0 or 2.0 mm/s. They calculated a force per unit area of the penetration tip and found a strong correlation of the penetration force to other methods of measuring strength, including compressive strength. This method has proven rather pragmatic and useful as a strength monitoring method for determining slipping speed (Lloret Fritschi 2016).

Slow Penetration

Fast penetration tests are pointwise measurements, giving an indication of yield stress at a certain point in time and requiring multiple samples or sampling sites to form an adequate image of strength build-up for processing. Slow penetration tests, on the other hand, are distinguished by using a single sample and measurement to

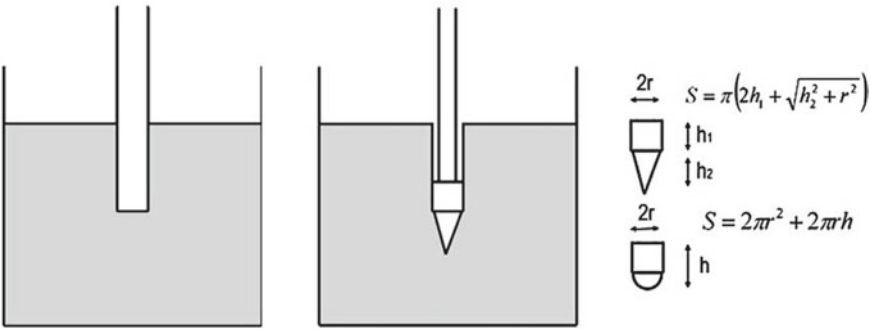

Fig. 4.12 Schematic of some penetration test geometries: Vicat needle (left) and penetration test (right). The load-bearing surface of the test depicted on the right is constant over time and is the basis for most penetration tests, with varying tip geometries. Figure from Lootens et al. (2009)

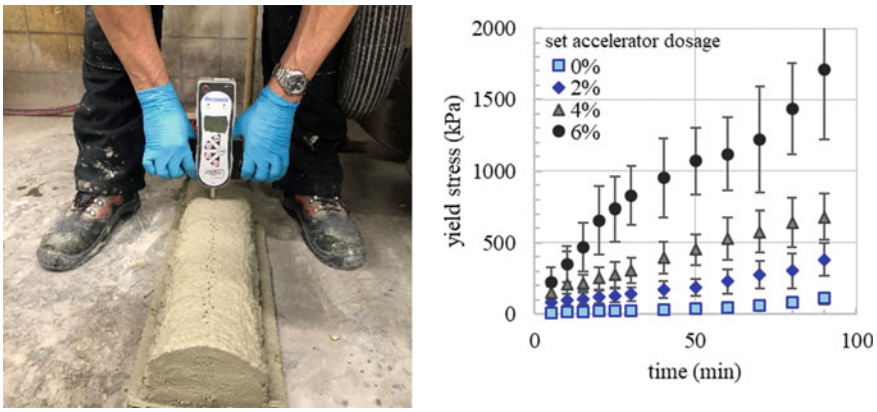

Fig. 4.13 (left) Fast penetration test on a SC3DP sample using a shotcrete penetrometer, (right) results of fast penetration tests showing the effect of set accelerator dosage (0, 2, 4 and 6% bwoc—by weight of cement) on the yield stress evolution (Dressler et al. 2020)

monitor the structural build-up over an entire processing time window. These slow penetration tests are performed by having a needle penetrating the paste or mortar only once at a very slow speed. During the slow penetration test, a force is measured as a function of the penetration depth. Since the yield stress of the material mainly influences the force during penetration, the penetration resistance of a tool can be considered as a rheological measurement. Compared to the fast penetration test, the slow one has several advantages. Firstly, the material is measured under static and unsheared conditions. In a fast penetration test, it must be ensured that the resulting cylindrical volume of the penetrated tool in the sample does not affect subsequent measurements. In addition, the material is affected by the permanent movement of the instrument before and after penetration due to vibrations. These problems do not occur with a slow penetration test.

A slow penetration test cannot be performed with every device. Successful performance depends on how precisely a device can perform slow movements and simultaneously measure small changes in force. With some experience, such a penetrometer can be custom made (Pott et al. 2020) (Fig. 4.14a). Otherwise, commercially manufactured systems can be purchased (example in Fig. 4.14b).

Figure 4.15 shows the results of three penetration tests—one mortar and two cement pastes at different penetration speeds. For this investigation, a spherical tool was used as a penetration tip (Fig. 14b). It can be seen that with different speeds and different maximum forces, different durations of hydration can be stated and that different materials can be investigated. Moreover, the slow penetration test is a suitable method for testing paste-rich printable mortars.

The handling is straightforward and fast, and the results are well reproducible. The method is well suited for testing the hydration process of different mortars (Reiter et al. 2020; Lootens et al. 2009; Pott et al. 2020; Reiter 2019). The measured force can be used to calculate the yield stress of the material. Lootens et al. (2009) give

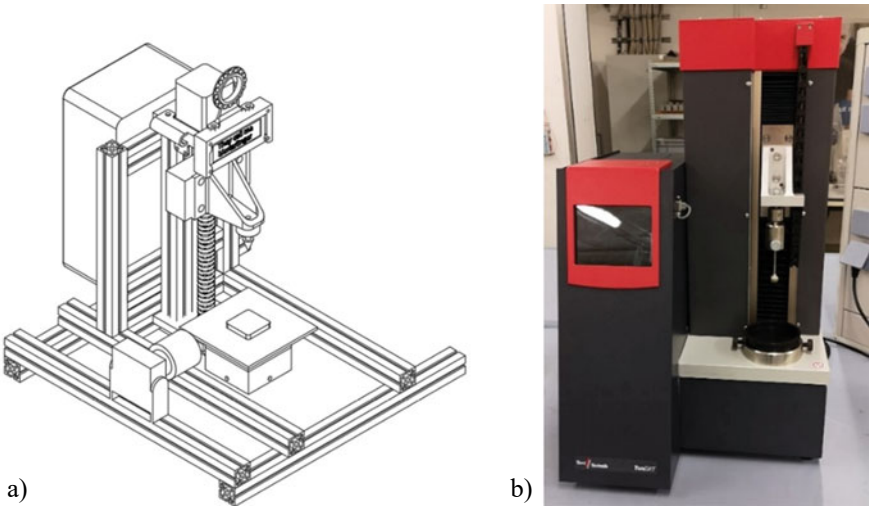

Fig. 4.14 **a** Custom-made penetrometer at TU Berlin **b** Penetrometer of the company Toni Technik with a spherical tool

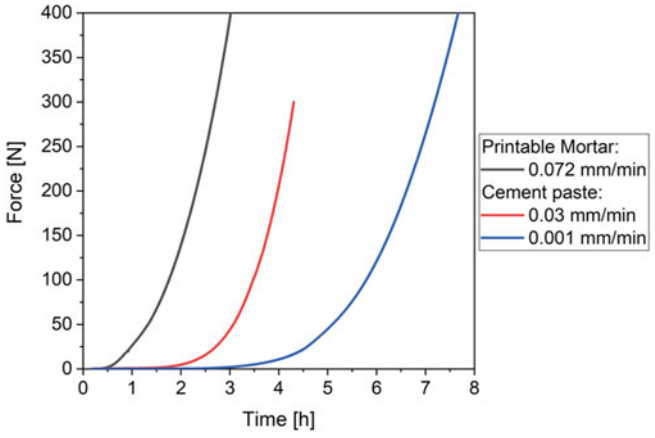

Fig. 4.15 Results of a slow penetration test of a cement paste (CEM I) and a printable mortar with a w/b-ratio of 0.36 at penetration speeds of 0.072, 0.03 and 0.001 mm/min

formulas for different penetration tips/configurations. However, these formulae must be used with caution, as the calculated yield stress depends only on the measured force and the shear surface. The investigations of the authors have shown that bodies with the same shell surface, but different geometries do not show the same force and, therefore, the calculation would not give the same yield stress for the same material. Further optimisations for the yield stress calculation via the penetration test are therefore desirable.

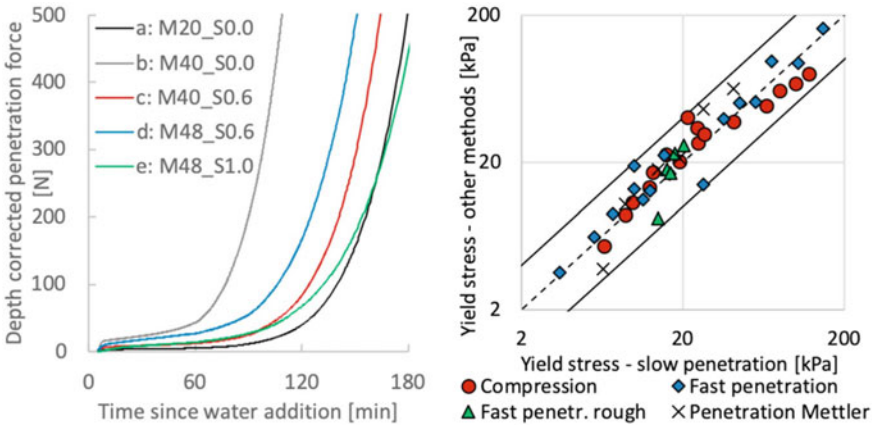

Fig. 4.16 (left) penetration force over time for mortars. The nomenclature Mx_Sy refers to x = sand content and y = superplasticizer dosage. (right) Yield stress calculated from penetration force using best fit N_C and its correlation to other methods. Solid lines give the 0.5–2 × range of expected values. Figures from Reiter et al. (2020)

Recent work by Reiter (2019) and Reiter et al. (2020) detail a similar slow penetration test, but modelled as a geomechanical soil stability problem. More specifically, the penetration force can be related to the yield stress for plastic materials through the use of a bearing capacity factor N_C, which is an analytically or empirically derived value relating stress at the penetration tip σ_f to the cohesion c_0, which is then related to the yield stress. This relation, based on soil mechanical considerations, can also be adapted to take into account minor effects such as surcharge, soil weight, heave, and cone bluntness, which can be considered depending on the penetration test setup. They used a universal testing machine setup, which drove a needle at a speed of 20.0 mm/h while continuously measuring the penetration force. The penetration tip had a cone geometry with a height of 30 mm and a radius of 10 mm. Some results for mortars are shown in Fig. 4.16, showing the strong effect of volume content of solids (sand content) in yield stress increase, as well as the two regimes of yield stress increase: an initial, slow evolution in yield stress followed by an exponential increase associated with the onset of hydration and the growth of hydration products. In the same figure, one can also observe that this penetration force, through a best fit bearing capacity factor N_C, compares favorably with other yield stress measurement methods such as compression and fast penetration. The method has also been successfully adapted to both slipforming and layered extrusion digital fabrication processes, seen in Fig. 4.17.

As it has been stated before, this method offers numerous advantages, especially the advantage of a single measurement which, with a proper setup, can give accurate yield stress evolution over a time span of hours, thus covering the time period of relevance for most digital fabrication processes. The analysis of Reiter (2019) demonstrates that the penetration tip geometry is a crucial factor as well, as using this

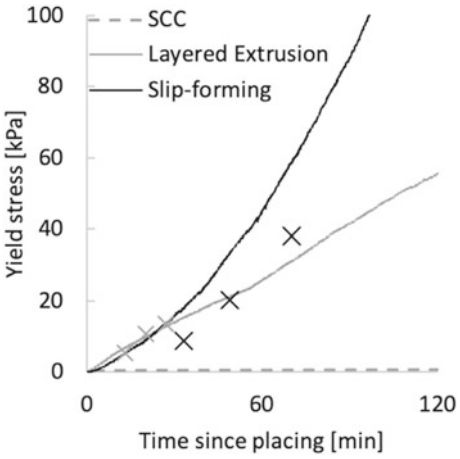

Fig. 4.17 Penetration (solid lines) and yield stress from compressive strength (crosses) for two different digital fabrication mortars, one for layered extrusion and one for slipforming. Also included is a retarded SCC, showing no increase in yield stress over time. Figure from Reiter et al. (2020)

soil mechanical approach demonstrates that the shearing surface does not occur on the penetration tip surface, but rather at a surface away from the tip, in homogeneous, previously unsheared material, and therefore can be considered a true static yield stress of the material.

The method is reliable for giving continuous, accurate yield stress measurements for mortars, but it does have certain limitations. The briefly described soil mechanical approach shows linearity between penetration force and the cohesion for plastic materials not dominated by frictional contacts between aggregate particles. When frictional contacts begin to dominate, then the friction angle must be considered, and this cannot be determined by the penetration test. Generally, however, digital fabrication mortars are paste-rich and can be considered as plastic materials over the ranges of relevance for processing, about 1–200 kPa. Reiter et al. (2020) cautions, however, that the method does not detect when this transition to a frictional material occurs, so materials of unknown compositions may require some cross-correlation between the slow penetration method with more established discrete methods such as compression. Reiter et al. (2020) also describes other issues with the method that must be dealt with carefully, such as the possibility of wall slip at the container edges leading to a lower penetration force, thus the container size must be selected appropriately to avoid this.

4.4.2.7 Measurements for Slipforming

In the special case of slipforming, a formwork smaller than the element being produced slides upward and a cementitious material exits the formwork with enough strength to support itself and the material above it (Lloret et al. 2015; Lloret Fritschi 2016). The process success hinges on ensuring the concrete has enough strength at the exit, but not so much that the friction between the concrete and the formwork

causes the material to tear off. Friction measurements have been demonstrated by the use of force sensors mounted to the formwork that measure a global friction force (Schultheiss et al. 2016) and an upper bound of material strength (and lower bound on the slipping speed) established by ensuring that through measurement of the volume of concrete in the formwork, a force balance can be calculated to ensure that there is no tensile stress at the exit (Lloret et al. 2017) and the risk of fracture is minimised.

More difficult is the measurement of the structural build-up within the bulk of the material inside the formwork, which determines if the material has enough strength to avoid collapse. Generally, as pointed out earlier, this is done by taking some similar material aside and performing penetration tests over time. In Lloret et al. (2017), however, it was shown that a small deformable membrane near the exit of the formwork could be used to measure the formwork pressure dilatometrically. With this measurement, one can provide a reasonable estimate of the material yield stress at the exit point of the formwork, which would give a lower bound on the material strength (and upper bound on slipping speed) for process success.

Craipeau et al. (2019) introduced a novel measurement in which pore water pressure, measured via a special gauge attached to the formwork, was correlated to shear stress at the formwork/material interface. These results showed that the pore water transition from pressure to suction correlates well with the material's structuration and the transition from the liquid to the solid state. This method offers another possibility for process monitoring of digitally controlled slipforming processes.

4.5 Indirect Methods: Calorimetry

As discussed in this chapter, the mechanical strength of cementitious binders in the fresh and hardening state is related to a physical microstructure, generated via two processes: flocculation of particles and the formation of hydration products. The earlier sections in this chapter have been devoted to direct measures of mechanical properties, either destructive or non-destructive. However, other methods can be correlated to the measurement of strength and can also potentially prove simpler to measure, lending themselves better to in-situ monitoring, and they are briefly discussed in this section. These methods are chemical in nature as well, as opposed to direct destructive or non-destructive mechanical methods, which were detailed earlier. The most widely used of these methods is calorimetry.

Calorimetry is the measurement of heat and heat production, and it is a general way of studying processes, including cement hydration, being used as a standard technique now for decades (Bensted 1987). The processes that underly cement hydration generate heat, and the heat generated is proportional to the amount of hydration products formed, and thus to the strength. The most common calorimetric techniques are (1) (semi)-adiabatic calorimetry and (2) isothermal calorimetry (Wadsö et al. 2016). Adiabatic calorimetry methods involve the direct measurement of temperature

evolution of an insulated sample over time, while heat losses to the environment, which occur in reality, should be accounted for (thus the "semi-" prefix). Isothermal calorimetry methods directly measure the thermal power (heat production) in a sample. More detailed information is available from isothermal calorimetry, and thus it is the more widely used method for research purposes. However, (semi)-adiabatic calorimetry finds more utility in the field and on-site applications due to the fact that larger sample sizes, including coarse aggregates, can be used.

A typical heat evolution curve has been shown in Fig. 4.2, where the important time periods in the hydration of cement are shown and detailed in Sect. 4.3.2 of this chapter. While all zones should be of importance to any process with cementitious materials, the most critical zone for 3D printed materials is right at the boundary of Zones II and III, where the onset of the acceleration period begins, as this coincides with where setting occurs—the transformation of the material from a fluid, shapeable material, to a solid material. One can imagine that following a calorimetry curve and following when the curve begins to increase at the onset of the acceleration period would give a useful processing parameter. Nonetheless, initial developments of set-on-demand systems for Smart Dynamic Casting (Shahab et al. 2014) demonstrated little correlation between mechanical strength build-up for process success and isothermal calorimetry curves. The same study, however, did note that isothermal calorimetry was a useful tool for process development in terms of giving indications of accelerator and retarder effectiveness. Hence, at this point, it is not advised to use calorimetry methods for in situ process monitoring to make predictions of strength for digital concrete processing. However, more recent developments in accelerator systems that give a very strong initial heat signal, in particular ettringite based systems (Sect. 4.3.3), may allow this to be revisited.

4.6 Robustness and Quality Control

RILEM TC 228-MPS (Khayat and Schutter 2014) defines robustness of SCC as 'The characteristic of a mixture that encompasses its tolerance to variations in constituent characteristics and quantities, variations during concrete mixing, transport, and placement, as well as environmental conditions.' Although rheological characteristics of SCC are also very relevant for 3D-printed concrete, other characteristics such as elasticity in the fresh state or structuration rate also have to be considered. A general definition of robustness of 3D-printed concrete can be derived from the definition of robustness of SCC from Van Der Vurst et al. (2017): The robustness of 3D-printed concrete is the capacity to retain its required rheological parameters despite small variations in mix proportioning, material properties and production method. This definition focuses on the robustness of a material against internal and external influences in order to achieve and maintain the required properties in fresh state. Besides the material robustness, a process robustness can also be assessed and/or improved. More generally spoken, the variation in relevant

Table 4.1 Sources of variation for concrete strength and rheological characteristics

Source of variation	Source specification
Material	Variations in characteristics of cement, supplementary materials, fine aggregates (silt, grading), coarse aggregates (dust, bond), admixtures
Manufacturing	Variation in ingredient weights (water, cementitious materials, admixture), mixing, transporting, delivery time, temperature, air content, workability

production aspects has to be sufficiently low or to be compensated for to achieve the ambitioned quality of a printed object.

Obla (2015) listed sources of concrete strength variation. The same parameters are expected to affect the characteristics of 3D-printed concrete in the fresh state (Table 4.1).

For Ready-mix concretes produced in traditional concrete plants, it is now accepted that the most sensitive parameter is the final water content of the mixture (Bonen et al. 2007). This parameter sensitivity finds its origin in the high flocculation of the aggregates' humidity, which is delicate to assess precisely in large stockpiles. As a result, the accuracy in both water and sand content dosage is weaker than the ones of any other components as shown in Fig. 4.18.

However, printable materials seem today to be often used under the form of pre-mixed bags (dry mortars). All components are then fully dried, and the main robustness issue of ready-mix concrete might be expected to vanish.

Moreover, the production tools for printing facilities are expected to involve lower capacities mixers as the required material consumption per hour is extremely low compared to a standard concrete casting phase. With lower volume batches, all weighting equipment are still to be invented or at least chosen. It is therefore, at

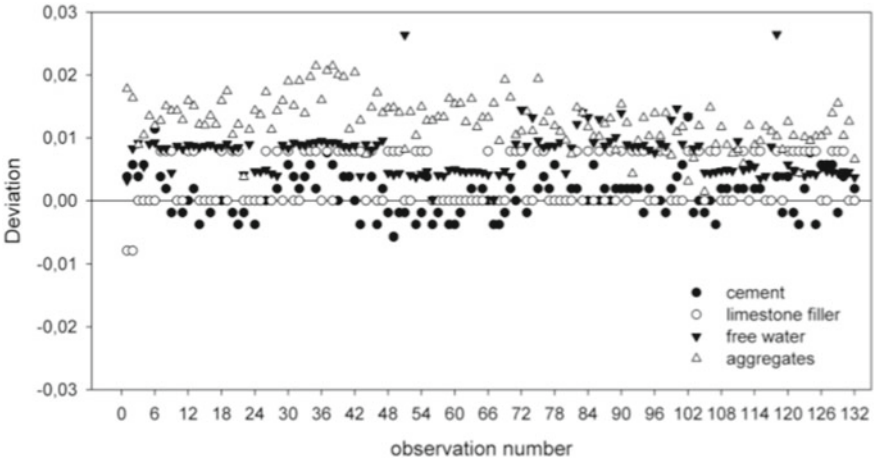

Fig. 4.18 Observed deviations of constituent materials during one week of concrete production in a precast factory. Figure from Nunes (2008)

this stage, extremely tricky to anticipate if the most sensitive component will be water (like standard concrete), the pre-mix powder or the accelerating additive.

As printable materials are mostly defined by their ability to build up a structure and increase their cohesion/yield stress with time, it means that they are expected to be extremely sensitive to the silicate/aluminate balance and to the admixture/cement interactions. Both are, in turn, expected to be sensitive to dissolution and precipitation processes at extremely early stage along with sulfate availability. However, binders used in the design of printable mixtures (cement, fillers and additives) may more or less vary in their size distribution, shape, porosity, mineral composition and content of secondary chemical components such as sulfates. Availability and delivery capacity of cement factories are major reasons for changes in raw materials or product characteristics.

Cement (i.e. clinker and sulfate carriers) variation is, therefore, expected, at this stage of 3D printing technological development, to have the most important effect on the robustness fresh properties of printable concrete in fresh and hardened states.

4.7 Summary

This chapter focuses on the measurement of fresh properties for cementitious materials in digital fabrication processes. The determination of these properties, and especially their monitoring over time, is critical for processing success. The strength/yield stress/cohesion and the elastic modulus, as well as how they evolve with time (often called structural build-up) are primary among fresh state properties. The importance of these has been briefly discussed in this chapter, as well as the background chemistry and the methods of using chemical admixtures to control these properties for digital fabrication processes.

Up until now, simple and robust techniques, such as the slump/spread flow test, as well as sensitive techniques, such as rheometry, exist for the measurement of these properties. However, recently, some have been specially developed or applied to printable cementitious materials for digital fabrication processes. These include techniques that can generate all important material parameters for processing, but require high investments in labour and material (such as triaxial compression) as well as techniques that require a single sample to monitor the yield stress over the entire process relevant time window (slow penetration).

It is important to emphasise that in the case of yield stress/strength/cohesion measurements, destructive tests are necessary, and other types of non-destructive tests require some assumptions and correlations to be made. This chapter is intended to give a spectrum of current possibilities for these measurements that can serve as starting points for further development as the field of digital fabrication with cementitious materials grows further.

Finally, it is important for the printing process to control the materials and to assess and understand the variation. It is not possible to provide robustness in all kind of scenarios and the worst conditions with regard to variation. Tailor-made concrete

requires experienced production personnel and adequate quality control, to a greater extent than existing ready mix plants. The selection of components and production process with low variation are key for the robust production with 3D-printed concrete.

References

Alfani, R., and Guerrini, G. L. (2005). Rheological test methods for the characterization of extrudable cement-based materials—a review. Materials and Structures, 38, 239–247.

Alfani, R., Grizzuti, N., Guerrini, G. L., Lezzi, G. (2007). The use of the capillary rheometer for the rheological evaluation of extrudable cement-based materials. Rheologica acta, 46, 703–709.

Assaad, J. J, Harb, J., Maalouf, Y. (2014). Measurement of yield stress of cement pastes using the direct shear test. Journal of Non-Newtonian Fluid Mechanics, 214, 18–27. https://doi.org/10.1016/j.jnnfm.2014.10.009.

Assaad, J., Khayat, K. H., and Mesbah, H. (2003a). Assessment of Thixotropy of Flowable and Self-Consolidating Concrete. MJ, 100, 99–107. https://doi.org/10.14359/12548.

Assaad, J., Khayat, K. H., and Mesbah, H. (2003b). Variation of Formwork Pressure with Thixotropy of Self-Consolidating Concrete. MJ, 100, 29–37. https://doi.org/10.14359/12460.

Barnes, H. A., and Nguyen, Q. D. (2001). Rotating vane rheometry—a review. Journal of Non-Newtonian Fluid Mechanics, 98, 1–14.

Banfill, P. F. G., and Kitching, D. R. (1990). 14 USE OF A CONTROLLED STRESS RHEOMETER TO STUDY THE YIELD STRESS OF OILWELL CEMENT SLURRIES. In: Rheology of Fresh Cement and Concrete: Proceedings of an International Conference, Liverpool, 1990. CRC Press, p. 125.

Benbow, J., and Bridgwater, J. (1993). Paste flow and extrusion. Oxford Series on Advanced Manufacturing, No. 10, Clarendon Press, Oxford.

Bensted, J. (1987). Some applications of conduction calorimetry to cement hydration. Advances in Cement Research, 1, 35–44. https://doi.org/10.1680/adcr.1987.1.1.35.

Bonen, Deshpande, Olek, Shen, L., Struble, L., Lange, D., and Khayat, K. (2007). Robustness of Self-Consolidating Concrete. In: Proceedings of the Fifth International RILEM Symposium on Self-compacting Concrete. Ghent, Belgium, pp 33–42.

Bouvet, A., Ghorbel, E., and Bennacer, R. (2010). The mini-conical slump flow test: Analysis and numerical study. Cement and Concrete Research, 40, 1517–1523.

C01 Committee Test Methods for Time of Setting of Hydraulic Cement by Vicat Needle. ASTM International.

C09 Committee Test Method for Time of Setting of Concrete Mixtures by Penetration Resistance. ASTM International.

Chan, T. W., and Baird, D. G. (2002). An evaluation of a squeeze flow rheometer for the rheological characterization of a filled polymer with a yield stress. Rheologica Acta, 41, 245–256.

Chen, Y., Li, Z., Chaves Figueiredo, S., Copuroglu, O., Veer, F., Schlangen, E. (2019). Limestone and Calcined Clay-Based Sustainable Cementitious Materials for 3D Concrete Printing: A Fundamental Study of Extrudability and Early-Age Strength Development. Applied Sciences, 9, 1809. https://doi.org/10.3390/app9091809.

Craipeau, T., Lecompte, T., Toussaint, F., and Perrot, A. (2019). Evolution of Concrete/Formwork Interface in Slipforming Process. In: Wangler, T., Flatt, R. J. (eds) First RILEM International Conference on Concrete and Digital Fabrication—Digital Concrete 2018. Springer International Publishing, pp. 12–23.

Choi, M., Roussel, N., Kim, Y., and Kim, J. (2013). Lubrication layer properties during concrete pumping. Cement and Concrete Research, 45, 69–78. https://doi.org/10.1016/j.cemconres.2012.11.001.

D18 Committee Test Method for Mechanical Cone Penetration Testing of Soils. ASTM International.
D18 Committee Test Method for Moisture Content Penetration Resistance Relationships of Fine-Grained Soils. ASTM International.
D18 Committee Test Method for Unconsolidated-Undrained Triaxial Compression Test on Cohesive Soils. ASTM International.
D18 Committee Test Method for Shear Testing of Bulk Solids Using the Jenike Shear Cell. ASTM International.
D18 Committee Test Method for Unconfined Compressive Strength of Cohesive Soil. ASTM International.
Dressler, I., Freund, N., and Lowke, D. (2020). The Effect of Accelerator Dosage on Fresh Concrete Properties and on Interlayer Strength in Shotcrete 3D Printing. Materials, 13, 374. https://doi.org/10.3390/ma13020374.
Drewniok, M., Cygan, G., and Gołaszewski, J. (2017). Influence of the Rheological Properties of SCC on the Formwork Pressure. Procedia Engineering, 192, 124–129.
De Larrard, F., Sedran, T., Hu, C., et al. (1996). Evolution of the workability of superplasticised concretes: assessment with the BTRHEOM rheometer. In: RILEM PROCEEDINGS, pp. 377–388.
EN 14488–2: Testing sprayed concrete—Part 2: Compressive strength of young sprayed concrete.
Engmann, J., Servais, C., and Burbidge, A. S. (2005). Squeeze flow theory and applications to rheometry: a review. Journal of Non-newtonian Fluid Mechanics, 132, 1–27.
Estellé, P., Lanos, C., Perrot, A., and Amziane, S. (2008). Processing the vane shear flow data from Couette analogy. Applied Rheology, 18, 34037.
Estellé, P., Lanos, C., and Perrot, A. (2008). Processing the Couette viscometry data using a Bingham approximation in shear rate calculation. Journal of Non-Newtonian Fluid Mechanics, 154, 31–38.
Estellé, P., and Lanos, C. (2012). High torque vane rheometer for concrete: principle and validation from rheological measurements. Applied Rheology, 22, 12881.
EN 206–1. Concrete - Part 1: Specification, performance, production and conformity.
Flatt, R. J., and Bowen, P. (2006). Yodel: A Yield Stress Model for Suspensions. Journal of the American Ceramic Society, 89, 1244–1256. https://doi.org/10.1111/j.1551-2916.2005.00888.x.
Ferraris, C. F., and de Larrard, F. (1998). Modified slump test to measure rheological parameters of fresh concrete. Cement, Concrete and Aggregates, 20, 241–247.
Feys, D., Cepuritis, R., Jacobsen, S, Lesage, K., Secrieru, E., and Yahia, A. (2018). Measuring rheological properties of cement pastes: most common techniques, procedures and challenges. RILEM Technical Letters, 2, 129–135.
Feys, D., Wallevik, J. E., Yahia, A., Khayat, K., and Wallevik, O. H. (2012). Extension of the Reiner–Riwlin equation to determine modified Bingham parameters measured in coaxial cylinders rheometers. Materials and Structures, 46, 289–311. https://doi.org/10.1617/s11527-012-9902-6.
Gelardi, G., and Flatt, R. J. (2016). 11 - Working mechanisms of water reducers and superplasticizers. In: Science and Technology of Concrete Admixtures. Woodhead Publishing, pp. 257–278.
Händle, F. (2007). Extrusion in ceramics. Springer Science & Business Media.
Hu, C., de Larrard, F., Sedran, T., Boulay, C., Bosc, F., and Deflorenne, F. (1996). Validation of BTRHEOM, the new rheometer for soft-to-fluid concrete. Materials and Structures, 29, 620–631.
Jayathilakage, R., Sanjayan, J., and Rajeev, P. (2019). Direct shear test for the assessment of rheological parameters of concrete for 3D printing applications. Mater Struct, 52, 12. https://doi.org/10.1617/s11527-019-1322-4.
Khalil, N., Aouad, G., El Cheikh, K., and Rémond, S. (2017). Use of calcium sulfoaluminate cements for setting control of 3D-printing mortars. Construction and Building Materials, 157, 382–391. https://doi.org/10.1016/j.conbuildmat.2017.09.109.
Khayat, K., Schutter, G. D. (2014). Mechanical Properties of Self-Compacting Concrete: State-of-the-Art Report of the RILEM Technical Committee 228-MPS on Mechanical Properties of Self-Compacting Concrete. Springer International Publishing.

Kloft, H., Krauss, H. –W., Hack, N., Herrmann, E., Neudecker, S., Varady, P. A., and Lowke, D. (2020). Influence of process parameters on the interlayer bond strength of concrete elements additive manufactured by Shotcrete 3D Printing (SC3DP). Cement and Concrete Research, 134, 106078. https://doi.org/10.1016/j.cemconres.2020.106078.

Koehler, E. P., Fowler, D. W., Ferraris, C. F., and Amziane, S. (2005). A new, portable rheometer for fresh self-consolidating concrete. ACI SPECIAL PUBLICATIONS, 233, 97.

Koehler, E. P., and Fowler, D. W. (2004). Development of a portable rheometer for fresh portland cement concrete. ICAR Research Report-105–3F, University of Texas at Austin.

Le Roy, R., and Roussel, N. (2005). The Marsh Cone as a viscometer: theoretical analysis and practical limits. Materials and Structures, 38, 25–30.

Lecompte, T., and Perrot, A. (2017). Non-linear modeling of yield stress increase due to SCC structural build-up at rest. Cement and Concrete Research, 92, 92–97. https://doi.org/10.1016/j.cemconres.2016.11.020.

Lee, H. K., Lee, K. M., Kim, Y. H., Yim, H., and Bae, D. B. (2004). Ultrasonic in-situ monitoring of setting process of high-performance concrete. Cement and Concrete Research, 34, 631–640. https://doi.org/10.1016/j.cemconres.2003.10.012.

Lloret Fritschi, E. (2016). Smart Dynamic Casting—A digital fabrication method for non-standard concrete structures. ETH Zurich.

Lloret, E., Shahab, A. R., Linus, M., Flatt, R. J., Gramazio, F., Kohler, M., and Langenberg, S. (2015). Complex concrete structures: Merging existing casting techniques with digital fabrication. Computer-Aided Design, 60, 40–49. https://doi.org/10.1016/j.cad.2014.02.011.

Lloret Fritschi, E., Reiter, L., Wangler, T., Gramazio, F., Kohler, M., and Flatt, R. J. (2017). Smart Dynamic Casting: Slipforming with Flexible Formwork—Inline Measurement and Control. In: Proceedings HPC/CIC Tromsø 2017. Norwegian Concrete Association, paper no. 27.

Lootens, D., Jousset, P., Martinie, L., Roussel, N., and Flatt, R. J. (2009). Yield stress during setting of cement pastes from penetration tests. Cement and Concrete Research, 39, 401–408. https://doi.org/10.1016/j.cemconres.2009.01.012.

Liu, S. H., Sun, D., and Matsuoka, H. (2005). On the interface friction in direct shear test. Computers and Geotechnics, 32, 317–325. https://doi.org/10.1016/j.compgeo.2005.05.002.

Mantellato, S., Palacios, M., and Flatt, R. J. (2019) Relating early hydration, specific surface and flow loss of cement pastes. Mater Struct, 52, 5. https://doi.org/10.1617/s11527-018-1304-y.

Marchon, D., and Flatt, R. J. (2016). 8 - Mechanisms of cement hydration. In: Aïtcin, P. –C., Flatt, R. J. (eds.) Science and Technology of Concrete Admixtures. Woodhead Publishing, pp. 129–145.

Marchon, D., Kawashima, S., Bessaies-Bey, H., Mantellato, S., and Ng, S. (2018). Hydration and rheology control of concrete for digital fabrication: Potential admixtures and cement chemistry. Cement and Concrete Research, 112, 96–110. https://doi.org/10.1016/j.cemconres.2018.05.014.

Ma, G., and Wang, L. (2018). A critical review of preparation design and workability measurement of concrete material for largescale 3D printing. Frontiers of Structural and Civil Engineering, 12, 382–400.

Mahaut, F., Mokéddem, S., Chateau, X., Roussel, N., and Ovarlez, G. (2008). Effect of coarse particle volume fraction on the yield stress and thixotropy of cementitious materials. Cement and Concrete Research, 38, 1276–1285. https://doi.org/10.1016/j.cemconres.2008.06.001.

Ma, S., Qian, Y., and Kawashima, S. (2018). Experimental and modeling study on the non-linear structural build-up of fresh cement pastes incorporating viscosity modifying admixtures. Cement and Concrete Research, 108, 1–9.

Mostafa, A. M., and Yahia, A. (2016). New approach to assess build-up of cement-based suspensions. Cement and Concrete Research, 85, 174–182. https://doi.org/10.1016/j.cemconres.2016.03.005.

Mimoune, M., and Aouadja F. Z. (2004). Rheometrical exploitation of experimental results obtained from new simulation device for extrusion on clay pastes. Materials and Structures, 37, 193–201.

Mechtcherine, V., Bos, F. P., Perrot, A., da Silva, W. R. L., Nerella, V. N., Fataei, S., Wolfs, R. J. M., Sonebi, M., and Roussel, N. (2020). Extrusion-based additive manufacturing with cement-based materials—Production steps, processes, and their underlying physics: A review. Cement and Concrete Research, 132, 106037. https://doi.org/10.1016/j.cemconres.2020.106037.

Mettler, L. K., Wittel, F. K., Flatt, R. J., and Herrmann, H. J. (2016). Evolution of strength and failure of SCC during early hydration. Cement and Concrete Research, 89, 288–296. https://doi.org/10.1016/j.cemconres.2016.09.004.

Myrdal, R. (2007). Accelerating admixtures for concrete. State of the art. SINTEF Building and Infrastructure; COIN - Concrete innovation Centre.

Nguyen, T. L. H., Roussel, N., and Coussot, P. (2006). Correlation between L-box test and rheological parameters of a homogeneous yield stress fluid. Cement and Concrete Research, 36, 1789–1796.

Nielsson, I., and Wallevik, O. H. (2003). Rheological evaluation of some empirical test methodspreliminary results. In: Third international RILEM symposium, RILEM Pub. PRO, pp. 59–68.

Nunes S. da C. B. (2008). Performance-based design of self-compacting concrete (SCC): A contribution to enchance SCC mixtures robustness. Ph.D., Universidade do Porto (Portugal).

Obla, K., Lobo, C. (2015). Prescriptive Specifications: A reality check. Concrete International, pp. 29–31.

Pashias, N., Boger, D. V., Summers, J., and Glenister, D. J. (1996). A fifty cent rheometer for yield stress measurement. Journal of Rheology, 40, 1179–1189.

Perrot, A., Rangeard, D., and Mélinge, Y. (2014). Prediction of the ram extrusion force of cement-based materials. Applied Rheology, 24, 53320.

Perrot, A., Mélinge, Y., Estellé, P., Rangeard, D., and Lanos, C. (2011). The back extrusion test as a technique for determining the rheological and tribological behaviour of yield stress fluids at low shear rates. Applied Rheology, 21, 53642.

Perrot, A., Mélinge, Y., Rangeard, D., Micaelli, F., Estelle, P., and Lanos, C. (2012). Use of ram extruder as a combined rheo-tribometer to study the behaviour of high yield stress fluids at low strain rate. Rheologica acta, 51, 743–754.

Perrot, A., Lecompte, T., Khelifi, H., Brumaud, C., Hot, J., and Roussel, N. (2012). Yield stress and bleeding of fresh cement pastes. Cement and Concrete Research, 42, 937–944. http://dx.doi.org/https://doi.org/10.1016/j.cemconres.2012.03.015.

Pierre, A., Perrot, A., Histace, A., Gharsalli, S., and Kadri, E. H. (2016). A study on the limitations of a vane rheometer for mineral suspensions using image processing. Rheologica Acta.

Pott, U., Ehm, C., Jakob, C., and Stephan, D. (2020). Investigation of the Early Cement Hydration with a New Penetration Test, Rheometry and In-Situ XRD. In: Mechtcherine, V., Khayat, K., and Secrieru, E. (eds.) Rheology and Processing of Construction Materials. Springer International Publishing, Cham, pp. 246–255.

Perrot, A., Rangeard, D., Nerella, V., and Mechtcherine, V. (2019). Extrusion of cement-based materials—an overview. RILEMTechLett 3. https://doi.org/10.21809/rilemtechlett.2018.75.

Pierre, A., Lanos, C., and Estellé, P. (2013). Extension of spread-slump formulae for yield stress evaluation. Applied Rheology, 23, 63849.

Qian, Y., and Kawashima, S. (2016). Use of creep recovery protocol to measure static yield stress and structural rebuilding of fresh cement pastes. Cement and Concrete Research, 90, 73–79.

Reiter, L., Wangler, T., Roussel, N., and Flatt, R. J. (2018). The role of early age structural build-up in digital fabrication with concrete. Cement and Concrete Research, 112, 86–95. https://doi.org/10.1016/j.cemconres.2018.05.011.

Reiter, L., Wangler, T., Anton, A., and Flatt, R. J. (2020). Setting on demand for digital concrete—Principles, measurements, chemistry, validation. Cement and Concrete Research, 132, 106047. https://doi.org/10.1016/j.cemconres.2020.106047.

Reiter, L. (2019). Structural Build-up for Digital Fabrication with Concrete—Materials, Methods, and Processes. ETH Zurich.

Reinhardt, H. W., Große, C. U., and Herb, A. T. (2000). Ultrasonic monitoring of setting and hardening of cement mortar—A new device. Mat Struct, 33, 581–583. https://doi.org/10.1007/BF02480539.

Roussel, N. (2006). A thixotropy model for fresh fluid concretes: Theory, validation and applications. Cement and Concrete Research, 36, 1797–1806. https://doi.org/10.1016/j.cemconres.2006.05.025.

Roussel, N., and Lanos, C. (2003). Plastic fluid flow parameters identification using a simple squeezing test. Applied Rheology, 13, 132–139.

Roussel, N., Lemaître, A., Flatt, R. J., and Coussot, P. (2010). Steady state flow of cement suspensions: A micromechanical state of the art. Cement and Concrete Research, 40, 77–84. https://doi.org/10.1016/j.cemconres.2009.08.026.

Roussel, N. (2007). The LCPC BOX: a cheap and simple technique for yield stress measurements of SCC. Materials and Structures, 40, 889–896.

Roussel, N. (2005). Steady and transient flow behaviour of fresh cement pastes. Cement and Concrete Research, 35, 1656–1664. https://doi.org/10.1016/j.cemconres.2004.08.001.

Roussel, N. (2006). A thixotropy model for fresh fluid concretes: Theory, validation and applications. Cement and Concrete Research, 36, 1797–1806. http://dx.doi.org/https://doi.org/10.1016/j.cemconres.2006.05.025.

Roussel, N. (2011). Understanding the rheology of concrete. Elsevier.

Roussel, N. (2018). Rheological requirements for printable concretes. Cement and Concrete Research, 112, 76–85. https://doi.org/10.1016/j.cemconres.2018.04.005.

Roussel, N., Bessaies-Bey, H., Kawashima, S., Vasilic, K., and Wolfs, R. J. M. (2019). Recent advances on yield stress and elasticity of fresh cement-based materials. Cement and Concrete Research, 124, 105798. https://doi.org/10.1016/j.cemconres.2019.105798.

Roussel, N., and Coussot, P. (2005). "Fifty-cent rheometer" for yield stress measurements: From slump to spreading flow. Journal of Rheology, 49, 705–718. http://dx.doi.org/https://doi.org/10.1122/1.1879041.

Roussel, N., Ovarlez, G., Garrault, S., and Brumaud, C. (2012). The origins of thixotropy of fresh cement pastes. Cement and Concrete Research, 42, 148–157. https://doi.org/10.1016/j.cemconres.2011.09.004.

Roussel, N., and Le Roy, R. (2005). The Marsh cone: a test or a rheological apparatus? Cement and Concrete Research, 35, 823–830.

Schultz, M. A., and Struble, L. J. (1993). Use of oscillatory shear to study flow behavior of fresh cement paste. Cement and Concrete Research, 23, 273–282.

Schutter, G. D., and Feys, D. (2016). Pumping of Fresh Concrete: Insights and Challenges. RILEM Technical Letters, 1, 76–80. https://doi.org/10.21809/rilemtechlett.2016.15.

Schultheiss, M., Wangler, T., Reiter, L., Roussel, N., and Flatt, R. J. (2016). Feedback control of Smart Dynamic Casting through formwork friction measurements. In: SCC 2016 - 8th International Rilem Symposium on Self-Compacting Concrete, Flowing toward Sustainability. RILEM Publications, pp. 637–644.

Shahab, A., Lloret, E., Fischer, P., Gramazio, F., Kohler, M., and Flatt, R. J. (2014). Smart dynamic casting or how to exploit the liquid to solid transition in cementitious materials. In: Proceedings CD of the 1st International Conference on Rheology and Processing of Construction Materials and of the 7th International Conference on Self-Compacting Concrete. Paris, France.

Spangenberg, J., Roussel, N., Hattel, J. H., Stang, H., Skocek, J., and Geiker, M.R. (2012). Flow induced particle migration in fresh concrete: theoretical frame, numerical simulations and experimental results on model fluids. Cement and Concrete Research, 42, 633–641.

Thomas, J. J., Jennings, H. M., and Chen, J. J. (2009). Influence of Nucleation Seeding on the Hydration Mechanisms of Tricalcium Silicate and Cement. J Phys Chem C, 113, 4327–4334. https://doi.org/10.1021/jp809811w.

Thrane, L. N., Pade, C., and Svensson, T. (2007). Estimation of Bingham rheological parameters of SCC from slump flow measurement. In: 5th International RILEM Symposium on Self-Compacting Concrete. RILEM Publications SARL, pp. 353–358.

Thrane, L. N., Pade, C., and Nielsen, C. V. (2009). Determination of rheology of self-consolidating concrete using the 4C-Rheometer and how to make use of the results. Journal of ASTM International, 7, 1–10.

Tchamba, J. C., Amziane, S., Ovarlez, G., and Roussel, N. (2008). Lateral stress exerted by fresh cement paste on formwork: Laboratory experiments. Cement and Concrete Research, 38, 459–466. http://dx.doi.org/https://doi.org/10.1016/j.cemconres.2007.11.013.

Toutou, Z., Roussel, N., and Lanos, C. (2005). The squeezing test: a tool to identify firm cement-based material's rheological behaviour and evaluate their extrusion ability. Cement and Concrete Research, 35, 1891–1899.

Trtnik, G., Turk, G., Kavčič, F., and Bosiljkov, V. B. (2008). Possibilities of using the ultrasonic wave transmission method to estimate initial setting time of cement paste. Cement and Concrete Research, 38, 1336–1342. https://doi.org/10.1016/j.cemconres.2008.08.003.

Thrane, L. N., Szabo, P., Geiker, M., Glavind, M., and Stang, H. (2004). Simulation of the test method "L-Box" for self-compacting concrete. Annual Transactions of the NORDIC rheology society, 12, 47–54.

Utsi, S., Emborg, M., and Carlsward, J. (2003). Relation between workability and rheological parameters. In: Third international RILEM symposium, RILEM Pub. PRO, pp. 154–164.

Van Der Vurst, F., Grünewald, S., Feys, D., Lesage, K., Vandewalle, L., Vantomme, J., De Schutter, G. (2017). Effect of the mix design on the robustness of fresh self-compacting concrete. Cement and Concrete Composites 82:190–201. https://doi.org/10.1016/j.cemconcomp.2017.06.005.

Wallevik, J. E. (2009). Rheological properties of cement paste: Thixotropic behavior and structural breakdown. Cement and Concrete Research, 39, 14–29. https://doi.org/10.1016/j.cemconres.2008.10.001.

Wallevik, J. E. (2006). Relationship between the Bingham parameters and slump. Cement and Concrete Research, 36, 1214–1221.

Wangler, T., Lloret, E., Reiter, L., Hack, N., Kohler, M., Bernhard, M., Dillenburger, B., Buchli, J., Roussel, N., and Flatt, R. J. (2016). Digital Concrete: Opportunities and Challenges. RILEM Technical Letters, 1, 67–75. https://doi.org/10.21809/rilemtechlett.2016.16.

Wolfs, R. J. M., Bos, F. P., and Salet, T. A. M. (2018). Early age mechanical behaviour of 3D printed concrete: Numerical modelling and experimental testing. Cement and Concrete Research, 106, 103–116. https://doi.org/10.1016/j.cemconres.2018.02.001.

Wallevik, J. E. (2008). Minimizing end-effects in the coaxial cylinders viscometer: Viscoplastic flow inside the ConTec BML Viscometer 3. Journal of Non-Newtonian Fluid Mechanics, 155, 116–123.

Wallevik, J. E. (2015). Parallel Plate Based Measuring System for the ConTec Viscometer–Rheological Measurement of Concrete with Dmax 32 mm. Nordic Concrete 50.

Wallevik, J. E. (2003). Rheology of particle suspensions: fresh concrete, mortar and cement paste with various types of lignosulfonates. Fakultet for ingeniørvitenskap og teknologi.

Wallevik, J. E. (2016). Development of parallel plate-based measuring system for the ConTec viscometer. Newsletter.

Wallevik, O. H., Feys, D., Wallevik, J. E., and Khayat, K. H. (2015). Avoiding inaccurate interpretations of rheological measurements for cement-based materials. Cement and Concrete Research, 78, 100–109.

Wolfs, R. J. M., Bos, F. P., and Salet, T. A. M. (2019). Triaxial compression testing on early age concrete for numerical analysis of 3D concrete printing. Cement and Concrete Composites, 104, 103344. https://doi.org/10.1016/j.cemconcomp.2019.103344.

Wolfs, R. J. M., Bos, F. P., and Salet, T. A. M. (2018). Correlation between destructive compression tests and non-destructive ultrasonic measurements on early age 3D printed concrete. Construction and Building Materials, 181, 447–454. https://doi.org/10.1016/j.conbuildmat.2018.06.060.

Wadsö, L., Winnefeld, F., Riding, K., Sandberg, P. (2016). Calorimetry. In: A Practical Guide to Microstructural Analysis of Cementitious Materials. CRC Press, pp. 56–93.

Yammine, J., Chaouche, M., Guerinet, M., Moranville, M., and Roussel, N. (2008). From ordinary rhelogy concrete to self compacting concrete: A transition between frictional and hydrodynamic

interactions. Cement and Concrete Research, 38, 890–896. https://doi.org/10.1016/j.cemconres.2008.03.011.

Yang, M., Neubauer, C. M., and Jennings, H. M. (1997). Interparticle potential and sedimentation behavior of cement suspensions: Review and results from paste. Advanced Cement Based Materials, 5, 1–7. https://doi.org/10.1016/S1065-7355(97)90009-2.

Yuan, Q., Zhou, D., Khayat, K. H., Feys, D., and Shi, C. (2017). On the measurement of evolution of structural build-up of cement paste with time by static yield stress test vs. small amplitude oscillatory shear test. Cement and Concrete Research, 99, 183–189.

Zhou, X., and Li, Z. (2005). Characterization of rheology of fresh fiber reinforced cementitious composites through ram extrusion. Materials and structures, 38, 17–24.

Zhou, X., Li, Z., Fan, M., and Chen, H. (2013). Rheology of semi-solid fresh cement pastes and mortars in orifice extrusion. Cement and Concrete Composites, 37, 304–311.

Zhou, Z., Solomon, M. J., Scales, P. J., and Boger, D. V. (1999). The yield stress of concentrated flocculated suspensions of size distributed particles. Journal of Rheology, 43, 651–671. https://doi.org/10.1122/1.551029.